Theory of Transition-Metal Complexes: Unrestricted Hartree–Fock Molecular-Orbital Method and Its Application to $KNiF_3$†

D. E. ELLIS*

Solid State and Molecular Theory Group, Massachusetts Institute of Technology, Cambridge, Massachusetts and Department of Physics, University of Florida, Gainesville, Florida

AND

A. J. FREEMAN‡

Francis Bitter National Magnet Laboratory,§ Massachusetts Institute of Technology, Cambridge, Massachusetts

AND

P. ROS¶

Solid State and Molecular Theory Group, Massachusetts Institute of Technology, Cambridge, Massachusetts

(Received 15 December 1967)

The unrestricted Hartree-Fock molecular-orbital self-consistent-field (MO-SCF) method is developed and applied to the problem of transition-metal ion clusters. This method removes many of the shortcomings of earlier treatments and provides, in principle, a framework for obtaining fairly accurate and meaningful results. Model calculations are reported for the $KNiF_3$ system, in which all matrix elements of the Hamiltonian are accurately computed (by the choice of a special one-center basis set) for all the electrons of the molecular cluster. Considerable variational freedom is allowed in all representations; as a consequence, significant covalent mixing is found for representations containing the metal $3s$ and $3p$ orbitals. This molecular-orbital approach thus differs greatly from the previous approach of using molecular orbitals formed as linear combination of atomic orbitals (MO-LCAO); in particular, it is emphasized that the simple (and inadequate) *single*-variational-parameter LCAO treatment of earlier calculations is replaced by full HF-SCF calculations in a multielectron framework including all electrons (and not just the bonding and antibonding electrons as in earlier treatments). Complete SCF calculations are carried out for both the $(NiF_6)^{4-}$ and the $(Ni_2F)^{3+}$ clusters (representing the metal-ion and the ligand-ion point of view, respectively) including the effects of an external crystalline field. Although these first (crude) calculations suffer from limited basis size, reasonable agreement with experiment is found for such quantities as the optical-splitting parameter $10Dq$, the transferred hyperfine interaction, and the neutron magnetic form factor.

I. INTRODUCTION

THE transition-metal salts have aroused great interest because of the wealth of unexplained experimental information obtained in recent years by optical, nuclear-magnetic-resonance, neutron-diffraction, and other techniques. A major stimulus has been the realization that a theoretical understanding of these observations might be important to the development of a theory of superexchange needed to explain the antiferromagnetism of these systems. Since analysis of the experimental data emphasized the importance of the role played by the magnetically inert anions, or ligand atoms, theoretical emphasis has concentrated heavily on attempts at understanding the behavior and properties of a cluster of atoms, the cluster considered as being representative of the crystal. This cluster was taken as a single metal ion and its nearest-neighbor ligands—the so-called ligand-field-theory approximation as opposed to the earlier, more naive single-ion, or crystal-field-theory approach. In this framework, Anderson[1] has stressed the importance of this cluster approach to the calculation of the exchange coupling between the magnetic open-shell metal ions (which are next-nearest neighbors to one another), i.e., the "superexchange" interaction.

Semiempirical molecular-orbital theories have already been applied to a large number of transition-metal complexes and the results confirm general trends observed in the electronic spectra and ionization potentials.[2] Unfortunately, the results of detailed theoretical calculations using the molecular-orbital (MO) approach have, as yet, not lived up to expectation. A system of special interest has been the antiferromagnetic compound $KNiF_3$. The early calculations of Sugano and Shulman[3] on the $(NiF_6)^{4-}$ cluster in $KNiF_3$ set a new standard for the *ab initio* one-electron treatment of metal complexes; however, some important questions remained to be answered. Among these were

(1) How does one extend the one- and two-electron

† Part of this work represents a thesis submitted by D.E.E. to the Physics Department, MIT, in partial fulfillment of the requirements for the Ph.D. degree, June 1966. Part of this work was supported by the National Science Foundation.

* Permanent address: Department of Physics, University of Florida, Gainesville, Fla.

‡ Permanent address: Department of Physics, Northwestern University, Evanston, Ill.

§ Supported by the U.S. Air Force Office of Scientific Research.

¶ Permanent address: Koninklijke/Shell-Laboratorium, Amsterdam, (Shell Research, N.V.), The Netherlands.

[1] P. W. Anderson, Solid State Phys. **14**, 99 (1963).

[2] H. Basch, A. Viste, and H. B. Gray, J. Chem. Phys. **44**, 10 (1966).

[3] S. Sugano and R. G. Shulman, Phys. Rev. **130**, 517 (1963).

MO models to a many-electron framework in a rigorous and consistent manner?[4]

(2) Does the difference of one-electron energies give an adequate approximation to cluster excitation energies, or do rearrangement and other "many-body" effects play an important role?

(3) To what extent are results affected by approximations to matrix elements and limited variational freedom?

(4) How strongly do ligand electrons interact with each other, and what is the effect of allowing s-p hybridization to take place?

(5) Is a spherical-well approximation to the crystalline potential adequate?

(6) What is the spin density in this $S=1$ system, and how do the spin-split orbitals differ?

Some of these questions were attacked by Nieuwpoort in a study of the metal carbonyls,[5] in which spin-restricted Hartree-Fock molecular-orbital self-consistent-field MO-SCF variational calculations were carried out on the $S=0$ ground states of the isolated complexes. This work showed that considerable rearrangement takes place during the approach to self-consistency starting from the free-atom charge densities. Ligand-s-p and ligand-ligand mixing were found to be important, as well as covalent mixing with, and distortions of, the metal orbitals. A net transfer of charge to the metal was observed. While these calculations represented a considerable advance over previous efforts, they were still limited by the use of a "frozen-core" approximation to the inner-shell orbitals, the use of some approximations to multicenter molecular integrals, and the restriction to doubly occupied orbitals. In addition, no excited states were calculated, so that one could only estimate excitation energies from the one-electron levels.

In this paper we apply the unrestricted Hartree-Fock, single-determinant, MO-SCF method to $(NiF_6)^{4-}$ and $(Ni_2F)^{3+}$ clusters in $KNiF_3$ as a natural extension of previous work. As a device for calculating all matrix elements accurately we introduce a one-center basis with some novel properties. Metal-core orbitals have been included in self-consistent calculations on the $^3A_{2g}$ and $^3T_{2g}$ states of the octahedral complex in the crystal field computed for $KNiF_3$. The triatomic cluster is used to study the F^{19} transferred hyperfine interaction. With the limited basis sets and the single-determinant approximation employed in this work, we cannot hope to resolve fully the questions discussed above. However, the calculated physical properties are reasonable and the results give some indication of the relative importance of various effects; for example, spin-polarization effects are found to be very large compared to the external crystalline field.

[4] R. E. Watson and A. J. Freeman, Phys. Rev. **134**, A1526 (1964); E. Simanek and Z. Sroubek, Phys. Status Solidi **4**, 251 (1964).

[5] W. C. Nieuwpoort, Philips Res. Repts. Suppl. No. 6 (1965).

Recently, the Heitler-London approach, as well as its extension to what has been called the "independent-bonding" scheme, has been used for these calculations.[6] In this alternative approach, the interaction between metal-ligand pairs is discussed in the language of configuration interaction. In our view, this treatment is made somewhat doubtful by the close proximity and resulting interaction of ligands with each other. For this reason we prefer to pursue the molecular-orbital approach, which includes all such interactions, with the ultimate aim of performing realistic *ab initio* configuration-interaction calculations. (We discuss the Heitler-London approach along with our own results in Sec. VII.)

In Sec. II we briefly review the Hartree-Fock equations for open-shell systems, and the approximations inherent to the cluster model. The basis functions and computing techniques used in these calculations are presented in Sec. III. A series of calculations which display the effect of various approximations is reported in Sec. IV, and the calculated crystal-field splitting and hyperfine parameters are given in Sec. V. Neutron magnetic scattering factors are reported in Sec. VI, and the role of covalency is illustrated.

II. APPLICATION OF THE HARTREE-FOCK METHOD TO AN IONIC CRYSTAL

In the Hartree-Fock theory of many-electron systems (extensively described in standard reference works[7]) an approximate N-electron wave function may be given by the single determinant

$$\Psi(1, 2, \cdots, N) = (N!)^{-1/2}\mathcal{A}\psi_1(1)\psi_2(2)\cdots\psi_N(N), \tag{2.1}$$

where $\mathcal{A}$ is the antisymmetrizing operator. Generally, the one-electron spin orbitals ψ_i are chosen as an orthonormal set of functions and written in the assumed separable form as

$$\psi_i = \varphi_i(\mathbf{r})\chi_i(s), \tag{2.2}$$

where the φ_i are functions of space coordinates only, and the χ_i used here are restricted to be spin eigenfunctions with eigenvalues of s_z equal to $\pm\frac{1}{2}$. The "best" spin orbitals are determined by minimizing the total energy of the system subject to variation of the φ_i.

In the LCAO (linear combination of atomic orbitals) approach[8] the spatial functions φ_i are approximated by a linear combination of basis functions, which for convenience are also chosen as an orthonormal set:

$$\varphi_i(\mathbf{r}) = \sum_j C_{ji}a_j(\mathbf{r}) \qquad \begin{matrix} i=1, 2, \cdots, N \\ j=1, 2, \cdots, M \end{matrix} \tag{2.3}$$

[6] E.g., J. Hubbard, D. E. Rimmer, and F. R. A. Hopgood, Proc. Phys. Soc. (London) **88**, 13 (1966).

[7] J. C. Slater, *Quantum Theory of Atomic Structure* (McGraw-Hill Book Co., New York, 1960), Vol. 1; R. K. Nesbet, Rev. Mod. Phys. **33**, 28 (1961).

[8] C. C. J. Roothaan, Rev. Mod. Phys. **23**, 69 (1951).

or in matrix notation

$$\varphi = a\mathsf{C}, \tag{2.4}$$

so that the columns of C form a discrete representation of the orbitals. One may immediately partition the matrix C into submatrices for either spin:

$$\mathsf{C} = \mathsf{C}^{\uparrow} + \mathsf{C}^{\downarrow}, \tag{2.5}$$

where $\mathsf{C}^{\uparrow}$ contains n spatial orbitals, each associated with a spin function χ with $s_z = +\frac{1}{2}$; $\mathsf{C}^{\downarrow}$ contains m orbitals with $s_z = -\frac{1}{2}$, and $n+m=N$. It is convenient to use the coefficient density matrices defined by

$$\rho_{ij}^{\uparrow} = \sum_{k}^{\text{occ}} C_{ik}^{\uparrow *} C_{jk}^{\uparrow} \tag{2.6}$$

and similarly for $\varrho^{\downarrow}$.

The Hartree-Fock equations for the spin orbitals ψ_i may be obtained by minimizing the total energy and are found to be

$$h_{\text{eff}}(1)\psi_i(1) = \epsilon_i \psi_i(1), \tag{2.7}$$

where

$$h_{\text{eff}} = -\tfrac{1}{2}\nabla_1^2 - \sum_g \frac{Z_g}{r_{1g}} + \int dv_2 \sum_k^{\text{occ}} \psi_k^*(2) \frac{1-P_{12}}{r_{12}} \psi_k(2), \tag{2.8}$$

and the integration is over both space and spin coordinates. The index g denotes the various nuclei of the system. The familiar operator P_{12} permutes coordinates of electrons 1 and 2. Substitution of Eq. (2.3) into (2.7), multiplication by a basis function $a_k^*(1)$, and integration of (2.7) lead to a set of equations for the coefficients C_{ij} which may be written in matrix form as

$$\mathsf{F}^{\uparrow}\mathsf{C}^{\uparrow} = \mathsf{C}^{\uparrow}\boldsymbol{\varepsilon}^{\uparrow}, \tag{2.9}$$

where $\boldsymbol{\varepsilon}^{\uparrow}$ is the diagonal matrix of the $\epsilon_i^{\uparrow}$, and

$$\mathsf{F}_{\uparrow} = \mathsf{H} + \mathsf{J}_{\downarrow} + \mathsf{J}_{\uparrow} - \mathsf{K}_{\uparrow} \tag{2.10}$$

and similarly for spin $\downarrow$. Here

$$H_{ij} = \int dv_1 a_i^*(1) \left(-\tfrac{1}{2}\nabla^2 - \sum_g \frac{Z_g}{r_{1g}}\right) a_j(1), \tag{2.11a}$$

$$J_{ij}^{\uparrow} = \int dv_1 a_i^*(1) \left(\sum_{k,l} \rho_{kl}^{\uparrow} \frac{a_k^*(2)a_l(2)}{r_{12}}\right) a_j(1), \tag{2.11b}$$

$$K_{ij}^{\uparrow} = \int dv_1 a_i^*(1) \left(\sum_{k,l} \rho_{k,l}^{\uparrow} \frac{a_k^*(2)a_l(1)}{r_{12}}\right) a_j(2). \tag{2.11c}$$

The Eqs. (2.9) must be solved for the unknown matrices C by an iterative procedure, since the F matrices depend upon C. Once the basis set $\{a\}$ is chosen and occupation numbers[9] specified, a self-consistent solution for the matrices C may be obtained by successive approximations to the matrices $\varrho^{\uparrow}$, $\varrho^{\downarrow}$ by using the C matrices obtained in the previous iteration.[10] The total electronic energy of the system can be expressed as

$$E^{\text{tot}} = (\varrho^{\uparrow}+\varrho^{\downarrow})\mathsf{H} + \tfrac{1}{2}(\varrho^{\uparrow}+\varrho^{\downarrow})(\mathsf{J}^{\uparrow}+\mathsf{J}^{\downarrow}) - \tfrac{1}{2}(\varrho^{\uparrow}\mathsf{K}^{\uparrow}+\varrho^{\downarrow}\mathsf{K}^{\downarrow}). \tag{2.12}$$

Since for crystalline systems the number of electrons N, and hence the dimension of the matrices in Eq. (2.9), is extremely large, we apply a well-known partitioning technique.[11] Instead of simultaneously diagonalizing the entire F matrix (of dimension $M \times M$), we may work with a subset of equations (2.9). One may divide the C and $\boldsymbol{\varepsilon}$ matrices as follows:

$$(\mathsf{F})(\mathsf{C}_m \mid \mathsf{C}_{M-m}) = (\mathsf{C}_m \mid \mathsf{C}_{M-m}) \left(\begin{array}{c|c} \boldsymbol{\varepsilon}_m & 0 \\ \hline 0 & \boldsymbol{\varepsilon}_{M-m} \end{array}\right), \tag{2.13a}$$

with the corresponding equations

$$\mathsf{F}\mathsf{C}_m = \mathsf{C}_m\boldsymbol{\varepsilon}_m, \qquad \mathsf{F}\mathsf{C}_{M-m} = \mathsf{C}_{M-m}\boldsymbol{\varepsilon}_{M-m}, \tag{2.13b}$$

and since the matrix C is unitary, we may perform unitary transformations within the submatrix C_m to lower the total energy (provided that the number of occupied orbitals in C_m is less than m) and to improve the approximate eigenfunctions without violating the orthogonality requirements. For perfect crystals the C matrix is cyclic and an obvious partitioning is present; however, we may choose any convenient partition containing the orbitals of some molecular cluster. Now we may consider a further partition of the C_m matrix such as

$$\left(\begin{array}{c|c} \mathsf{F}_{aa} & \mathsf{F}_{ab} \\ \hline \mathsf{F}_{ba} & \mathsf{F}_{bb} \end{array}\right)\begin{pmatrix} \mathsf{C}_{am} \\ \mathsf{C}_{bm} \end{pmatrix} = \begin{pmatrix} \mathsf{C}_{am} \\ \mathsf{C}_{bm} \end{pmatrix}(\boldsymbol{\varepsilon}_m), \tag{2.13c}$$

with the corresponding equations (dropping the subscript m)

$$\mathsf{F}_{aa}\mathsf{C}_a + \mathsf{F}_{ab}\mathsf{C}_b = \mathsf{C}_a\boldsymbol{\varepsilon}, \tag{2.13d}$$

$$\mathsf{F}_{ba}\mathsf{C}_a + \mathsf{F}_{bb}\mathsf{C}_b = \mathsf{C}_b\boldsymbol{\varepsilon}. \tag{2.13e}$$

Substitution of Eq. (2.13e) in (2.13d) gives the formal solution

$$\mathsf{F}_{aa}'\mathsf{C}_a = \mathsf{C}_a\boldsymbol{\varepsilon}, \tag{2.14}$$

[9] It is convenient to redefine the density matrices as $\rho_{ij} = \Sigma_k n_k C_{ik}^* C_{jk}$ in terms of the occupation numbers n_k, where the the sum now runs over all k. In this way one may control the number of electrons of either spin and, where symmetry partitioning is employed, the number of electrons in each representation. Furthermore, various configuration averages can be taken, making use of fractional n_k.

[10] R. K. Nesbet, Rev. Mod. Phys. **35**, 552 (1963); J. A. Pople and R. K. Nesbet, J. Chem. Phys. **22**, 571 (1954).

[11] P.-O. Löwdin, J. Mol. Spectry. **14**, 112 (1964).

where

$$\mathbf{F}_{aa}'=\mathbf{F}_{aa}+\mathbf{F}_{ab}\mathbf{C}_b(\mathbf{C}_b\boldsymbol{\varepsilon}-\mathbf{F}_{bb}\mathbf{C}_b)^{-1}\mathbf{F}_{ba} \qquad (2.15)$$

provided that the inverse of $(\mathbf{C}_b\boldsymbol{\varepsilon}-\mathbf{F}_{bb}\mathbf{C}_b)$ exists.

In the case of a crystal like $KNiF_3$ one can make a calculation on a $(NiF_6)^{4-}$ cluster from that crystal by making the partitioning of the matrix $\mathbf{C}$ so that $\mathbf{C}_m$ describes all orbitals (occupied and virtual) in the cluster and $\mathbf{C}_{M-m}$ describes all orbitals in the rest of the crystal. In addition, we choose $\mathbf{C}_a$ to contain only those basis functions a_j localized at the cluster. The second term of $\mathbf{F}_{aa}'$ in Eq. (2.15) then describes the overlap-mixing effects between the cluster and the rest of the crystal. It is easy to show[12] that this term is of order γ^2, where γ is the mixing parameter between basis functions on neighboring ions. In highly ionic crystals (such as $KNiF_3$) and with the use of a localized basis, the overlaps, and hence γ, will be small. We therefore will neglect all effects of the second term of Eq. (2.15), which is equivalent to the assumption $\mathbf{C}_b=0$. With these approximations Eq. (2.14) becomes

$$(\mathbf{F}_{aa}''-\boldsymbol{\varepsilon}_a')\mathbf{C}_a'=0. \qquad (2.14')$$

Here all matrices have the dimension $m\times m$, where m is the number of basis functions a_j localized at the cluster.

The matrix $\mathbf{F}_{aa}''$ now may be split into the Hartree-Fock matrix for the isolated cluster and terms giving interactions of the cluster with the rest of the crystal:

$$=\mathbf{F}_{aa}''=\mathbf{F}_a^{\text{cluster}}+V_{\text{cryst}}, \qquad (2.16)$$

with

$$(V_{\text{cryst}})_{ij}=\left\langle a_i\left|-\sum_\alpha\frac{Z_\alpha}{r_{1\alpha}}\right.\right.$$
$$\left.\left.+\int dv_2\sum_\mu^{\text{ext}}\psi_\mu^*(2)\frac{1-P_{12}}{r_{12}}\psi_\mu(2)\,\right|\,a_j\right\rangle, \qquad (2.17)$$

where the sum α is over all nuclei outside of the cluster and μ runs over all electrons not belonging to the cluster. The approximation given by Eq. (2.16) corresponds to the treatment of an isolated cluster in the molecular field of the crystalline environment. In previous molecular-orbital calculations[3,4] on $KNiF_3$, the crystal field has been approximated by a uniform potential well. In the calculations to be reported, various approximations have been used for the matrix elements (2.17). These include:

(1) *Point ions* on crystal sites; Eq. (2.17) then simplifies to

$$V_{ij}=\langle a_i\,|\,-\sum_\alpha(Z_{\text{eff},\alpha}/r_{1\alpha})\,|\,a_j\rangle. \qquad (2.18)$$

(2) *Distributed ions* on crystal sites; in this case

$$V_{ij}=\langle a_i\,|\,-\sum_\alpha[(Z_{\text{eff},\alpha}/r_{1\alpha})-V_\alpha(r_{1\alpha})]\,|\,a_j\rangle, \qquad (2.19)$$

where $V_\alpha(r_{1\alpha})$ is a correction term to (2.18) due to the overlap of cluster- and neighboring ion-electron densities.

III. BASIS SETS FOR THE CLUSTER MODEL

The successive partitioning scheme begins essentially with the computation of free-ion approximate eigenfunctions. The compact form and the relatively easy computation of accurate matrix elements make the choice of an analytic basis set advantageous. Of various analytic basis sets in use, the exponential Slater basis has proved most accurate and reliable. These basis functions are of the form

$$a_{nlm\sigma}=N_{nlm}r^{n-1}e^{-\alpha r}P_l^m(\theta)\,S_m^\sigma(\varphi), \qquad (3.1)$$

where N is a normalization constant, P_l^m is the associated Legendre function, and S_m^σ is the (real) trigonometric function $\sin m\varphi$ or $\cos m\varphi$. For our purposes it will be convenient to choose all basis functions real. Tables of accurate wavefunctions in this basis for numerous atoms and ions have been published[13]; these tables can often provide good starting wave functions for more extensive calculations. Another advantage of the Slater basis appears when we consider multicenter molecular or crystalline systems. A *multicenter Slater basis set* can be formed, consisting of sets of the functions given in Eq. (3.1) centered at *each* nuclear site. This multicenter basis set can represent an orbital properly in the vicinity of every nucleus, and the overlap and mixing of different atomic sets can form an accurate representation of the internuclear region. In addition, one may easily analyze the resulting molecular wave functions in terms of distortions of the component atoms.[14]

By now a considerable number of small molecules have been treated, making use of multicenter Slater basis sets. These include diatomic molecules, and larger

[12] One can write the second term of Eq. (2.15) as $\mathbf{F}_{al}\mathbf{C}_b\mathbf{C}_a^{-1}$. We suppose that the basis functions a_j and the eigenfunctions ϕ_i are localized about lattice sites; then the $\mathbf{C}$ matrix may be placed in the following form:

$$\left(\begin{array}{cc|c|c}
\sim 1 & \sim\gamma & \sim\gamma^2 & \cdots \\
\sim\gamma & \sim 1 & \sim\gamma & \cdots \\
\hline
\sim\gamma^2 & \sim\gamma & \sim 1 & \cdots \\
\cdot & \sim\gamma^2 & \sim\gamma & \cdots \\
\cdot & & & \\
\cdot & \cdot & \cdot & \\
\cdot & \cdot & \cdot &
\end{array}\right),$$

where γ symbolizes mixing coefficients of the order of the overlap between adjacent atomic functions. Thus $\mathbf{C}_b$ consists of terms of order γ and higher. In the same way we see that $\mathbf{F}_{ab}$ contains terms of the same order, so that the product $\mathbf{F}_{ab}\mathbf{C}_b$ is of order γ^2. In principle, one has the basis for an inerative procedure in which additional rows are successively brought into the $\mathbf{C}_a$ matrix.

[13] E. Clementi, IBM J. Res. Develop Suppl. **9**, 2 (1965).

[14] In fact, covalency can only be rigorously defined in the case of limited variational procedures restricted to free-atom functions as a basis. This and the problem of unambiguously defining ionicity in a molecule can be resolved by a sensible convention, such as the Mulliken overlap population analysis.

systems such as H_2O, CH_4, C_2H_6, H_6, NH_3, and PH_4. The results clearly indicate that the "optimized minimal Slater basis" is an excellent approximation to the Hartree-Fock eigenfunction. In this basis one chooses a small number of functions at each center and systematically varies all screening constants and linear coefficients to obtain minimum energy. The small number of functions chosen is dictated by the complex and time-consuming evaluation of multicenter matrix elements. As methods for computing these integrals improve, we may include larger basis sets and treat more complex systems to higher accuracy.

The main criterion by which a molecular wave function is judged is usually a comparison with experimental binding energy and charge moments. The calculation of excited states and transitions between states is usually not sufficiently developed to allow meaningful comparisons. Another possible criterion is the comparison between molecular wave functions obtained from very different basis sets. The ability to compare wave functions directly instead of the expectation value of some operator would be very useful; to date few such comparisons have been made.

We have already mentioned that at present the computation of matrix elements for the multicenter Slater basis is complex and tedious.[15] In order to study reasonably large molecular systems, we are forced to compromise between accuracy of the Slater set and the amount of computer time available for calculation. To this end we propose a specialized one-center mixed basis[16] which is particularly suited to centro-symmetric systems. This basis set may be developed by referring to one of the basic techniques applied in evaluating multicenter matrix elements.

Consider the basic two-electron repulsion integral encountered in the multicenter Slater basis set. The most general (and most complex) of these is the four-center integral:

$$\langle AB \mid CD\rangle = \iint dv_1 dv_2 a_{n1,l1,m1,\sigma1}{}^*(\mathbf{r}_{A1}) \times a_{n2,l2}(\mathbf{r}_{B1})_{m2,\sigma2}(1/r_{12})\, a_{n3,l3,m3,\sigma3}{}^*(\mathbf{r}_{C2}) \times a_{n4,l4,m4,\sigma4}(\mathbf{r}_{D2}). \quad (3.2)$$

In this notation $\mathbf{r}_{A1}$ means the coordinate vector of electron 1 measured from an origin at nucleus A. A general method for evaluating this and other multicenter integrals is to expand the integrand about some common origin in spherical harmonics. The angular and radial integrals may then be computed separately, thus reducing the order of quadrature required. The price of this simplification is that a series must usually be summed to evaluate the integral, and in the four-center case a doubly infinite series results. The two basic expansions required for this method are the potential expansion

$$r_{12}{}^{-1} = \sum_{J=0}^{\infty} \delta_J(r_{A1}, r_{A2})\, P_J{}^0(A; 1, 2), \quad (3.3)$$

where $\delta_J(r_{A1}, r_{A2}) = r_<{}^J / r_>{}^{J+1}$, and $P_J{}^0(A; 1, 2)$ is a Legendre function whose argument is the angle between $\mathbf{r}_1$ and $\mathbf{r}_2$, and the orbital expansion

$$a_{nlm\sigma}(\mathbf{r}_{B1}) = N_{nlm} \sum_{\lambda=m}^{\infty} (2\lambda+1) \times \eta_{nlm;\,\lambda}(\alpha, r_{A1}, R_{AB})\, P_\lambda{}^m(\theta_{A1})\, S_m{}^\sigma(\varphi_{A1}). \quad (3.4)$$

In both cases we have taken the final coordinate center to be at site A, with the local coordinate systems aligned on the AB axis. The final step of the procedure is to rotate all functions into a common coordinate system and to truncate sums according to vector coupling rules derived from the angular integral. In practice all remaining infinite sums are truncated at some finite angular momentum, say $l=20$, to obtain some desired accuracy in the integral. The angular integrals to be evaluated within these sums are products of three spherical harmonics, and can be computed in terms of well-known vector coupling coefficients and rotation matrix elements. The double-radial integrand consists of products of radial Slater functions (if the origin coincides with a nucleus), orbital expansion functions $\eta_{nlm;\,\lambda}$, and the potential function $\delta_J(r_{A1}, r_{A2})$.

We may now remark on some of the properties of the orbital radial expansion functions $\eta_{nlm;\,\lambda}(\alpha, r_A, R)$. These functions possess a pronounced peak or node in the vicinity of the radius of the generating Slater orbital $a_{nlm}(\mathbf{r}_B)$. The individual functions η are somewhat more extended toward the expansion origin, and the convergence rate of the series depends strongly on the parameter αR_{AB} (α is the exponential screening constant). In a severely truncated series, say $\max(\lambda)=4$, the expansion (3.4) generates a rather diffuse function about center A.

This observation leads us to consider centro-symmetric systems, for which we might choose a multicenter Slater basis set. The usual procedure would be to form multicenter symmetry orbitals by taking linear combinations of basis functions. One might attempt to calculate symmetry-orbital matrix elements directly by developing expansions analogous to Eq. (3.4). However, this approach is not very fruitful, for by choosing the center of symmetry as the unique expansion origin one often encounters unfavorable convergence rates in the integral series. One alternative is to compute the unsymmetrized multicenter integrals separately, selecting the expansion origin for optimum convergence

[15] This has been one of the central numerical problems of molecular theory; indications of the present status of the problem appear, for example, in Ref. 42 and F. E. Harris and H. H. Michels, J. Chem. Phys. **45**, 116 (1966).

[16] A number of one-center bases have been employed in molecular calculations, including exponential and Gaussian functions as well as a few numerical applications; for example, B. D. Joshi, J. Chem. Phys. **47**, 2793 (1967). Manageable bases of this type have two defects: inability to represent the wave-function cusp at distant nuclei and slow convergence in localizing charge about these nuclei.

in each case. This is an annoying feature, since it becomes difficult to produce an efficient computing scheme, and considerable manipulation is required to symmetrize the raw integrals.

A second alternative is to abandon the multicenter Slater basis set, while attempting to retain some of its essential features. In expanding a single Slater function or a symmetry combination of functions about the central site, one always obtains the same radial functions $\eta_{nlm;\,\lambda}$. These functions are multiplied by *fixed* coefficients and specific combinations of spherical harmonics. An equally valid procedure is to consider the functions

$$b_{nlm;\,\lambda\mu\sigma}(\mathbf{r}_A)=\eta_{nlm;\,\lambda}(\alpha, r_A, R)P_\lambda^\mu(\theta_A)S_\mu^\sigma(\varphi_A) \quad (3.5)$$

as *independent* basis functions for the molecular system. It is clear that for a sufficiently large basis this set is at least as good as the multicenter Slater set, for it forms the natural expansion of the Slater functions. It can be superior since the linear coefficient of each b function is a free parameter. It may be hoped that this variational freedom will permit truncation of the basis in orbital momentum λ to lower values than that required to reproduce a given Slater function.

The mixed basis which we propose is thus $\{\Phi\}=\{a, b\}$ for centro-symmetric clusters, in which $\{a\}$ is a Slater basis set at the central site, and $\{b\}$ is a basis of expansion functions for each ligand shell. One advantage of this basis choice is that contact can be maintained with a specific atomic basis from which the $\{b\}$ set is derived. Details of an efficient computation scheme for treating this basis are given in Appendix A and all of our results are given in this basis.

IV. CLUSTER CALCULATIONS AND CRYSTAL-FIELD SPLITTING

The computation of the crystal-field splitting parameter, $10Dq$, has been a major goal of all previous cluster calculations. Within the Hartree-Fock scheme, Δ, or $10Dq$, may be defined as the energy difference between two independently calculated N-electron states. For $KNIF_3$, this is taken to be[17]

$$\Delta=E^{\text{tot}}({}^3T_{2g}\zeta)-E^{\text{tot}}({}^3A_{2g}), \quad (4.1)$$

corresponding to a vibronic electric-dipole transition.[18] While one might hope that (as has been done often in the past) the transition could be described simply in terms of the one-electron promotion energy $\epsilon_{t_{2g}}-\epsilon_{e_g}$, such, however, is not the case, for upon examination of the eigenvalues for either the ground state (A_{2g}) or excited state (T_{2g}) one finds a considerable discrepancy.

[17] We use the crystal-field notation ${}^{2S+1}\Gamma_\gamma$, where Γ is an irreducible representation of the symmetry group of the cluster and γ, if mentioned, indicates a specific basis component of Γ.

[18] A more rigorous calculation of the broad bands actually observed in octahedral complexes is not yet possible; for an excellent review of the situation see C. J. Ballhausen, *Introduction to Ligand Field Theory* (McGraw-Hill Book Co., New York, 1962).

TABLE I. Basis set for Ni^{2+} and NiF_6 calculations.

$R=3.79371$ (metal-ligand distance).

a functions					
a_{1g}:	$1s$	$\alpha=27.8$			
	$2s$	12.5	e_g:	$3d$	$\alpha=2.3$
	$3s$	4.0		$3d$	5.0
	$3s$	7.5	t_{2g}:	$3d$	2.3
t_{1u}:	$2p$	11.7		$3d$	5.0
	$3p$	3.6			
	$3p$	6.2			
b functions[a]					
a_{1g}:	$1s(0, 0)$	$\alpha=8.658$	t_{1u}:	$1s(1, 0)$	$\alpha=8.658$
	$2s(0, 0)$	2.493		$2s(1, 0)$	2.493
	$2p_\sigma(0, 0)$	2.344		$2p_\sigma(1, 0)$	2.344
e_g:	$1s(2, 0)$	8.658		$2p_\pi(1, 0)$	6.0
	$2s(2, 0)$	2.493		$2p_\pi(1, 0)$	1.0
	$2p_\sigma(2, 0)$	2.344	t_{2g}:	$2p_\pi(2, -2)$	2.3
t_{1g}:	$2p_\pi(4, -4)$	2.2		$2p_\pi(2, -2)$	5.0
	$2p_\pi(4, -4)$	4.5	t_{2u}:	$2p_\pi(3, 2)$	2.2
				$3p_\pi(3, 2)$	4.5

[a] The eta functions are denoted as $nl(\lambda, \mu)$, where n and l are the atomic quantum numbers ($1s$, $2s$, $\cdots$), λ and μ are the angular quantum numbers of Eq. (3.5), and α is the screening parameter. μ may have several values for degenerate representations, in which case one representative value is given.

In fact, sufficient rearrangement takes place among *all* orbitals of the system after the excitation to have a net appreciable effect on the value of Δ. The result is not surprising, and is merely an indication of the magnitude of "core-distortion" effects. In particular, the metal $3s$ and $3p$ orbitals are sufficiently extended that considerable overlap and covalent mixing with ligand orbitals is expected. One finds that s-p hybridization, the mixing of ligand s and $2p$ orbitals, plays a significant role in determining the cluster wave function.[19]

In this section we present a series of approximate cluster calculations for the cubic perovskite $KNiF_3$. A cubic cell of this crystal has the Ni ion in the body-centered position, the F ions at the center of the faces, and the K ions at the corners; the cell edge is taken[20] to be 4.014 Å (7.585 a.u.). We may consider that this system constitutes a severe test of the methods developed in this paper, particularly because of the presence of unpaired spins. One may begin by taking the crystal to be a collection of Ni^{2+}, F^-, and K^+ ions, with two holes in the e_g (Ni^{2+} $3d$) shell of the magnetic ion.

Three series of calculations were made. Two of these (A and B below) were done with coordinate origin at

[19] Similar conclusions were reached in a "frozen core" LCAO-MO calculation of very limited variational freedom: D. E. Ellis, MIT M.S. thesis, 1964 (unpublished); D. E. Ellis, A. J. Freeman: and R. E. Watson, *Proceedings of the International Conference on Magnetism, Nottingham, England, 1964* (The Institute of Physics and the Physical Society, Berkshire, 1965), p. 335.

[20] A. Okazaki and Y. Suemune, J. Phys. Soc. Japan **16**, 671 (1961).

TABLE II. SCF calculations for Ni^{2+}, with and without crystal field of $KNiF_3$. Accuracy in E_{elec}, 0.001: with crystal field, $\Delta=0.0059$ a.u. $=1295$ cm^{-1}. These results may be compared with the more extensive Ni^{2+} calculation by R. E. Watson and A. J. Freeman (Ref. 37), which gave a total energy -1506 a.u.

	Ni^{2+}-t^6e^2 No crystal field		Ni^{2+}-t^6e^2 With crystal field; no Madelung correction		Ni^{2+}-t^5e^3 No crystal field		Ni^{2+}-t^5e^3 With crystal field; no Madelung correction	
E_{elec}	-1499.7906		-1499.7991		-1499.7902		-1499.7932	
	spin α	β	α	β	α	β	α	β
$\epsilon(1a_{1g})$	-307.197	-307.197	-307.203	-307.202	-307.197	-307.196	-307.199	-307.198
$\epsilon(2a_{1g})$	-37.557	-37.491	-37.564	-37.497	-37.557	-37.491	-37.559	-37.493
$\epsilon(3a_{1g})$	-5.162	-4.970	-5.167	-4.974	-5.162	-4.970	-5.164	-4.971
$\epsilon(1eg\theta)$	-1.506	...	-1.511	...	-1.506	...	-1.508	...
$\epsilon(1eg\epsilon)$	-1.506	...	-1.511	...	-1.453	-1.368	-1.454	-1.369
$\epsilon(1t_{1u})$	-34.183	-34.129	-34.189	-34.135	-34.183	-34.129	-34.185	-34.131
$\epsilon(2t_{1u})$	-4.248	-3.994	-4.253	-3.998	-4.248	-3.994	-4.250	-3.996
$\epsilon(1t_{2g}\zeta)$	-1.453	-1.368	-1.459	-1.372	-1.506	...	-1.508	...
$\epsilon(1t_{2g}\xi,\eta)$	-1.453	-1.368	-1.459	-1.372	-1.453	-1.368	-1.456	-1.370

a Ni^{2+} site—the first with a partition including only the magnetic ion, and the second obtained by extending the partition to include the ligand shell of six F^- sites.

In order to have a meaningful comparison of results, the same one-center basis set was used for each series; it is given in Table I. The Slater functions (a functions) were obtained by truncating Clementi's basis[13] for Ni^{2+}; the eta functions (b functions) were obtained by a similar truncation of the F^- Slater basis set. This mixed basis is chosen so that for each representation of $(NiF_6)^{4-}$ having m occupied orbitals there are at least $m+1$ basis functions; thus we also obtain the "first excited (virtual) orbital" of each symmetry species.

In the third set of calculations (C below) the F^- ion was taken as origin for the cluster, and a basis set appropriate to this configuration was chosen.

A. Single-Magnetic-Ion Calculations

Spin-unrestricted single-determinant wave functions for the ground state (t^6e^2, $^3A_{2g}$) and first excited state (t^5e^3, $^3T_{2g}$) of the 26-electron Ni^{2+} partition were obtained with and without the crystal-field matrix elements. Spin-restricted pseudo-closed-shell calculations[21] were performed to obtain starting density matrices, and inspection of the open-shell results shows that considerable rearrangement takes place in the outer orbitals of each symmetry when the spin-restriction is dropped. Self-consistent iterations were carried to an accuracy of at least 0.001 a.u. in total energy in each case. No attempt was made to orthogonalize the Ni^{2+} orbitals to near neighbors although overlap contributions to the crystal field were included. A very small crystal-field splitting of 1300 cm^{-1} is found.[22] Limitations of space do not permit us to tabulate the eigenvectors obtained; the orbitals do not differ greatly from free-ion Ni^{2+} functions. Total energy and one-electron energies for occupied orbitals of either spin are given in Table II. The Madelung correction necessary for placing Ni^{2+} calculations in the crystal field on an absolute energy scale can be computed very easily.[23]

B. $(NiF_6)^{4-}$ Cluster Calculations

The second series of calculations were made for 74 electrons of the $(NiF_6)^{4-}$ cluster, with the F^- 1s electrons treated as ligand point charges. Coulomb interactions and overlaps with the free-ion 1s orbitals were computed; deviations of the Coulomb potential from the point-charge result were very small, and in view of the rather small basis used it was decided not to orthogonalize to these orbitals. This approximation has an effect only in the immediate vicinity of ligand nuclei; however, it does mean that the wave function and spin density will be poorly represented at these sites. This inability of the basis to form charge densities tightly bound to the ligand nuclei is no real obstacle, for when we are interested in fine details of ligand orbitals, we may simply move the partitioning origin to a ligand site and make a new calculation in that frame—an assertion verified by the $(Ni_2F)^{3+}$ calculation reported later.

The results of the (metal+ligand shell) $(NiF_6)^{4-}$ calculations are presented in Table III; as before, the overlapping crystal field is computed, but no attempt is made to orthogonalize to the near neighbors (K^+). It is often helpful to identify the cluster-symmetry orbitals with the free-ion orbitals from which they arise in the LCAO picture; a schematic representation of the one-electron energy levels is given in Fig. 1. Some of the one-electron orbitals obtained for the ground state $(t^6e^2)A_{2g}$ of $(NiF_6)^{4-}$ are plotted in Figs. 2–6; the tightly bound Ni^{2+} core orbitals are omitted for clarity, and the t_{2u}, t_{1g} (nonbonding ligand $p\pi$)

[21] Obtained by choosing fractional occupation numbers n_k among the e_g and t_{2g} orbitals to produce a spin and orbital singlet.

[22] It would be desirable to orthogonalize the basis at least to the first ligand shell orbitals, and this could produce a considerable change in Δ. This was *not* done, in order to keep the basis as small as possible.

[23] See the review article of M. P. Tosi, Solid State Phys. **16**, 1 (1964).

TABLE III. SCF calculations for $(NiF_6)^{4-}$, with and without $KNiF_3$ crystal field. Without crystal field, $\Delta = 0.0479$ a.u. $= 10\,500$ cm^{-1}. With crystal field, $\Delta = 0.0492$ a.u. $= 10\,800$ cm^{-1}. Accuracy in E_{elec}, 0.001.

	$(NiF_6)^{4-}$-t^6e^2 No crystal field		$(NiF_6)^{4-}$-t^6e^2 With crystal field; no Madelung correction		$(NiF_6)^{4-}$-t^5e^3 No crystal field		$(NiF_6)^{4-}$-t^5e^3 With crystal field; no Madelung correction	
E_{elec}	−2006.4418		−2006.1928		−2006.3939		−2006.1436	
	spin α	β	α	β	α	β	α	β
$\epsilon(1a_{1g})$	−305.247	−305.246	−305.239	−305.238	−305.274	−305.273	−305.270	−305.270
$\epsilon(2a_{1g})$	−35.627	−35.568	−35.620	−35.561	−35.657	−35.597	−35.654	−35.594
$\epsilon(3a_{1g})$	−3.292	−3.132	−3.287	−3.127	−3.328	−3.160	−3.325	−3.158
$\epsilon(4a_{1g})$	−0.276	−0.272	−0.275	−0.271	−0.280	−0.274	−0.278	−0.273
$\epsilon(5a_{1g})$	1.052	1.064	1.054	1.065	1.049	1.056	1.051	1.058
$\epsilon(1eg\theta)$	−1.023	−1.018	−1.018	−1.014	−1.027	−1.021	−1.022	−1.016
$\epsilon(2eg\theta)$	0.296	0.671	0.302	0.676	0.268	0.657	0.272	0.662
$\epsilon(3eg\theta)$	0.819	•••	0.825	•••	0.812	•••	0.817	•••
$\epsilon(1eg\epsilon)$	−1.023	−1.018	−1.018	−1.014	−1.021	−1.019	−1.016	−1.014
$\epsilon(2eg\epsilon)$	0.296	0.671	0.302	0.676	0.302	0.361	0.305	0.364
$\epsilon(3eg\epsilon)$	0.819	•••	0.825	•••	0.822	0.839	0.828	0.844
$\epsilon(1t_{1g})$	0.697	0.700	0.705	0.707	0.697	0.701	0.704	0.708
$\epsilon(1t_{1u})$	−32.252	−32.203	−32.245	−32.196	−32.297	−32.231	−32.276	−32.228
$\epsilon(2t_{1u})$	−2.368	−2.154	−2.362	−2.148	−2.398	−2.186	−2.394	−2.183
$\epsilon(3t_{1u})$	−0.182	−0.178	−0.180	−0.176	−0.186	−0.182	−0.184	−0.180
$\epsilon(4t_{1u})$	0.814	0.820	0.830	0.837	0.812	0.818	0.828	0.834
$\epsilon(5t_{1u})$	1.384	1.393	1.392	1.400	1.378	1.387	1.385	1.394
$\epsilon(1t_{2g}\zeta)$	0.392	0.455	0.397	0.460	0.313	0.727	0.315	0.727
$\epsilon(2t_{2g}\zeta)$	0.792	0.801	0.791	0.801	0.782	•••	0.781	•••
$\epsilon(1t_{2g}\xi, \eta)$	0.392	0.455	0.397	0.460	0.361	0.428	0.364	0.431
$\epsilon(2t_{2g}\xi, \eta)$	0.792	0.801	0.791	0.801	0.787	0.796	0.786	0.795
$\epsilon(1t_{2u})$	0.832	0.834	0.844	0.846	0.832	0.832	0.844	0.845

orbitals are not shown. The partially occupied e_g orbitals are plotted separately for either spin. Since the spin dependence of other representations is not very noticeable in a plot, only the majority-spin α orbitals are given.

In order to discuss the one-electron energy levels, we refer first to the Ni^{2+} results (Table II) where it is seen that energy differences between the spin-split $3d$ (e_g, t_{2g}) orbitals are quite sizable. For example, in the t^6e^2 configuration $\mathcal{E}[t_{2g}, \alpha] - \mathcal{E}[e_g, \alpha] = 0.05$ a.u. and $\mathcal{E}[t_{2g}, \beta] - \mathcal{E}[_{2g}, \alpha] = 0.09$ a.u. These energies are larger than the optical splitting $\Delta[\sim 0.04$ a.u.$]$ and appear to be a dominant factor in determining orbital occupancy both in the Ni^{2+} ion and the octahedral complex.

The pronounced spin splitting in e_g and t_{2g} orbitals of $(NiF_6)^{4-}$ makes a direct comparison with results of the traditional ligand field theory somewhat difficult. Upon examination of Table III and Figs. 4, 5, and 6, one sees that the character of the ground-state orbitals, in order of energy, is

t_{2g}: $3d$, $2p\pi$;

$e_g^{\uparrow}$: $2s$, $3d$, $2p\sigma$;

$e_g^{\downarrow}$: $2s$, $2p\sigma$, $3d$ (unoccupied).

Thus the occupied "metal $3d$" molecular orbitals lie lower than the "fluorine $2p$" orbitals in apparent contradiction with the traditional theory (but in agreement with the relative position of the free-ion levels). We are reluctant to assign any great importance to this inversion, first because of the very limited basis set used here, and second because it does not affect the outcome for physical observables. The latter observation follows from the fact that the *unoccupied* $3e_g$, β orbital does show predominantly $3d$ antibonding character as is expected in the traditional theory. The significance of the unoccupied e_g, β orbital to all observable quantities is discussed in detail in Ref. (4), and it is pointed out that one may perform arbitrary unitary transformations on the occupied orbitals without affecting properties of the N-electron determinantal wave function.

We refer to Table III to compare e_g and t_{2g} orbital energies of either spin for the t^6e^2 $^3A_{2g}$ state of $(NiF_6)^{4-}$ calculated in the crystal field. As can be seen, the e_g open shell is much more strongly split than in the Ni^{2+} ion, while the splitting in the nominally closed t_{2g} shell is about the same. The effect on the t_{2g} shell is merely to polarize the $3d$ orbitals, while the e_g shell undergoes an inversion of orbital levels as well.

A rough calculation shows that about 0.8 electron has been transferred onto the Ni ion, leaving a net charge of $+1.2$. In choosing orbital occupancy for the excited state, we are guided by the first unoccupied or virtual levels from the SCF results. The first virtual

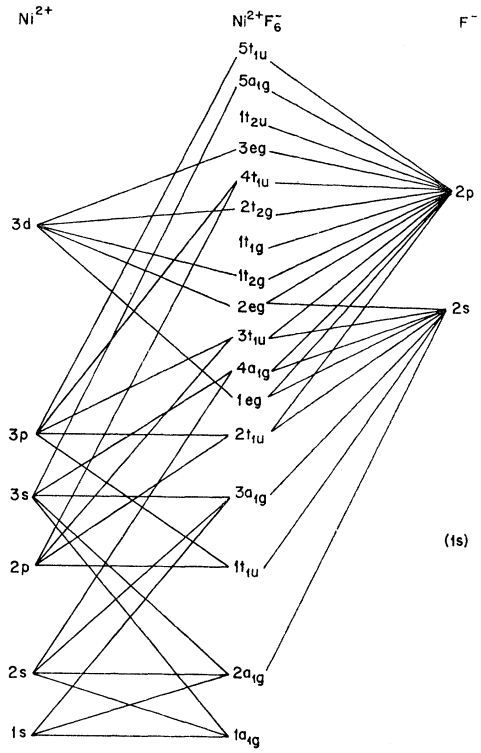

FIG. 1. MO energy levels for $(NiF_6)^{4-}$ cluster.

levels for β spin are

$$\begin{aligned} \mathcal{E}: \quad & 1.42\ 3e_g \quad 4.53\ 2t_{1g} \quad 12.20\ 6a_{1g}, \\ & 3.29\ 3t_{2g} \quad 4.68\ 2t_{2u} \\ & 3.52\ 4e_g \quad 5.02\ 6t_{1u} \end{aligned}$$

so promotion into $3e_g$ seems an obvious choice. From Table III it would appear that the $5a_{1g}$ or $5t_{1u}$ orbitals are least stable and could be easily chosen as donors for the excitation. However, this ordering may be due to the limited basis, so that we choose to promote a minority-spin electron from $t_{2g-\zeta}$ into the $3e_{g-\theta}$ hole to form the $^3T_{2g}$ state required by crystal-field theory. The self-consistent excited state was calculated with this choice of occupation numbers.

It is apparent that the external crystal field has had very little effect on the cluster wave function; the cubic-field splitting $E^{\text{tot}}(\cdots t^5e^3) - E^{\text{tot}}(\cdots t^6e^2) = \Delta$ is found to be 10 500 cm^{-1} for the isolated $(NiF_6)^{4-}$ cluster and 10 800 cm^{-1} in the crystal environment. The experimentally determined Δ is 7250 cm^{-1}.[24] It is interesting to note that although the crystal field is fairly large in the vicinity of the ligands, it undergoes considerable variation with both positive and negative regions, so that the largest matrix elements are 0.01 a.u. for ligand orbitals and an order of magnitude smaller for metal orbitals (excluding the Madelung term).

A detailed discussion of the crystal-field problem and its role in the cluster model is presented as Appendix B.

[24] K. Knox, R. G. Shulman, and S. Sugano, Phys. Rev. **130**, 512 (1963).

C. $(Ni_2F)^{3+}$ Calculations

In order to treat properties of the ligands, such as transferred hyperfine effects (to be discussed in the next section), we have carried out calculations in which the cluster has an F^- ion at its center. The simplest such cluster, composed of the triatomic system Ni^{2+}–F^-–Ni^{2+}, was chosen for this work. Although this triatomic system is but a crude approximation, it still allows us to discuss some of our results from the ligand "point of view" and to further test the cluster approximation.

For these crude cluster calculations the $(Ni_2F)^{3+}$ cluster with symmetry $D_{\infty h}$ (linear triatomic molecule Ni^{2+}–F^-–Ni^{2+}) was chosen, with the Ni^{2+} $1s$, $2s$, and $2p$ electrons treated as point charges. Thus the cluster wave function was taken to represent the 42 electrons drawn from the Ni^{2+} $3p$, $3s$, $3d$, and F^- $1s$, $2s$, and $2p$ shells. The basis set used is given in Table IV. The ferromagnetic configuration (also appropriate for the NMR experiments in the paramagnetic regime) was adopted, with four holes, all of β spin, assigned to the symmetry species a_{1g}, a_{1u}, e_{2g}, e_{2u}. The results of this calculation are presented in Table V and, while the metal orbitals are probably poor due to our point-charge approximation for the core, the wave function may be expected to be fairly accurate around the fluorine nucleus.

V. F^{19} TRANSFERRED HYPERFINE INTERACTION

In this section we shall be concerned with calculating the transferred hyperfine interaction at a single F^{19}

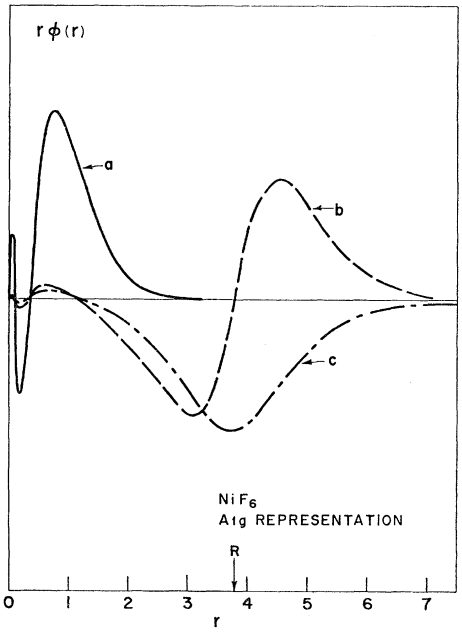

FIG. 2. NiF_6 a_{1g} representation. (a) $3a_{1g}$; (b) $4a_{1g}$; (c) $5a_{1g}$.

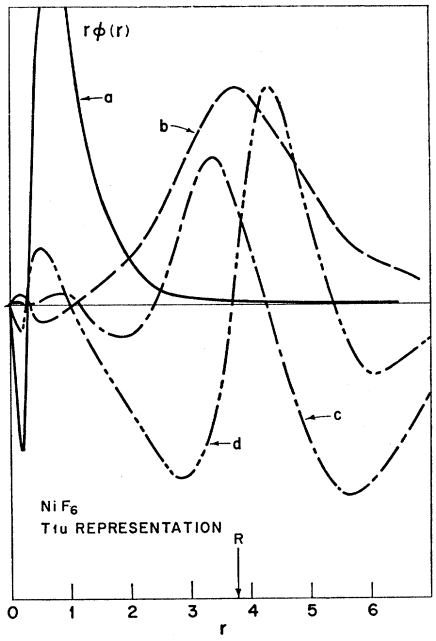

FIG. 3. NiF_6 t_{1u} representation. (a) $2t_{1u}$; (b) $3t_{1u}$; (c) $4t_{1u}$; (d) $5t_{1u}$.

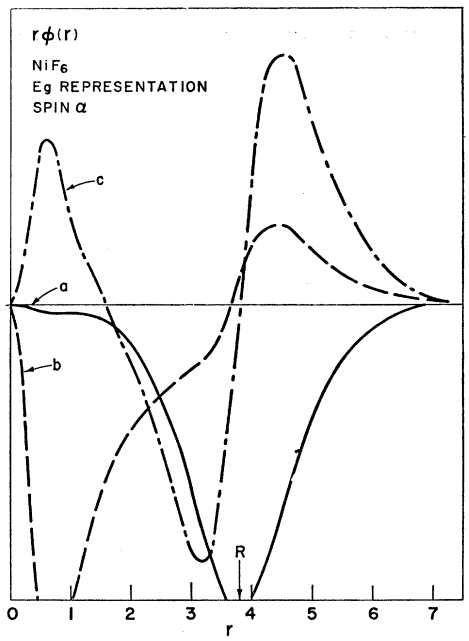

FIG. 5. NiF_6 e_g representation, spin α. (a) $1e_g$; (b) $2e_g$; (c) $3e_g$.

nucleus. Following a brief review of the theory, definitions are given for the parameters A_s, A_σ, and A_π within the molecular-orbital approach. Results calculated for the NiF_6 and Ni_2F clusters are discussed (in some detail in the latter case in order to emphasize the various contributions to the hyperfine interaction). It is found that the interaction calculated in NiF_6 is an order of magnitude too small compared with experiment, an effect due primarily to the very limited one-center basis used. Results for the triatomic case (Ni_2F) give a much larger interaction, and A_s in particular is found to be an order of magnitude larger than experiment. The error is attributed to the limited basis and the neglect of covalent effects of other ligands upon the metal ions.

The interaction energy of a single electron with the

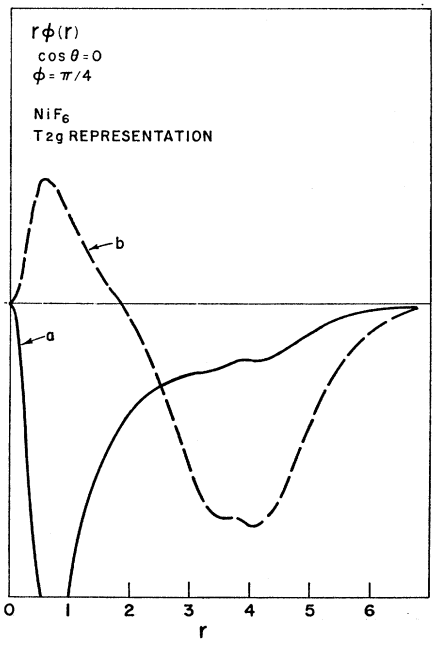

FIG. 4. NiF_6 t_{2g} representation. (a) $1t_{2g}$; (b) $2t_{2g}$.

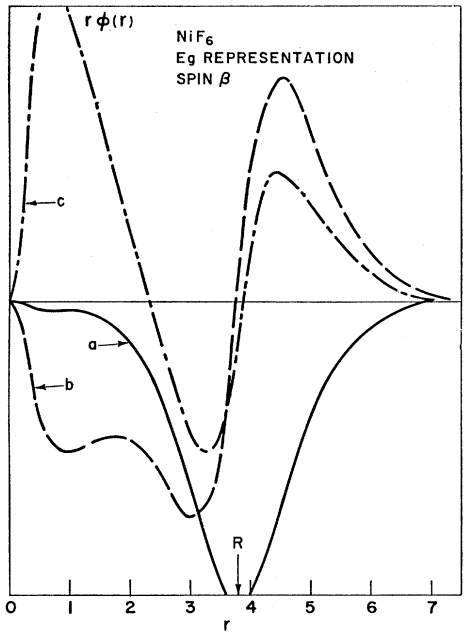

FIG. 6. NiF_6 e_g representation, spin β. (a) $1e_g$; (b) $2e_g$; (c) $3e_g$(unoccupied).

TABLE IV. Basis set Ni-F-Ni calculation.

a functions					
a_{1g}:	$1s$	$\alpha=$ 8.425			
	$2s$	11.384			
	$2s$	2.562			
a_{1u}:	$2p_\sigma$	1.511			
	$2p_\sigma$	3.834			
e_{1g}:	$2p_\pi$	1.511			
	$2p_\pi$	3.834			
b functions					
a_{1g}:	$3s(0,0)$	$\alpha=4.0$	e_{1u}:	$3p_\pi(2,1)$	$\alpha=3.6$
	$3p_\sigma(0,0)$	3.6		$3d_\pi(2,1)$	2.3
	$3d_\sigma(0,0)$	2.3		$3d_\pi(2,1)$	5.0
	$3d_\sigma(0,0)$	5.0			
a_{1u}:	$3s(1,0)$	4.0	e_{2g}:	$3d_\delta(2,2)$	2.3
	$3p_\sigma(1,0)$	3.6		$3d_\delta(2,2)$	5.0
	$3d_\sigma(1,0)$	2.3			
	$3d_\sigma(1,0)$	5.0	e_{2u}:	$3d_\delta(3,2)$	2.3
e_{1g}:	$3p_\pi(1,1)$	3.6		$3d_\delta(3,2)$	5.0
	$3d_\pi(1,1)$	2.3			
	$3d_\pi(1,1)$	5.0			

nuclear moment is given by[25]

$$W=g_e\beta\gamma_N\hbar\mathbf{I}_N\cdot\left(\frac{2}{g_e}\frac{1}{r^3}-\frac{\mathbf{s}}{r^3}+\frac{3\mathbf{r}(\mathbf{s}\cdot\mathbf{r})}{r^5}+\frac{8\pi}{3}\mathbf{s}\delta(\mathbf{r})\right), \tag{5.1}$$

which we may write as

$$W=-\gamma_N\hbar\mathbf{I}_N\cdot\mathbf{H}_{\text{eff}} \tag{5.2}$$

in terms of the effective magnetic field produced by the electron. Since we are primarily interested in the spin-spin interaction, we will drop the orbital term $1/r^3$ and write

$$\mathbf{H}_{\text{eff}}=\frac{g_e\beta}{a_0^3}\left(\frac{\mathbf{s}}{r^3}-\frac{3\mathbf{r}(\mathbf{s}\cdot\mathbf{r})}{r^5}-\frac{8\pi}{3}\mathbf{s}\delta(\mathbf{r})\right), \tag{5.3}$$

where $\beta=e\hbar/2mc=-0.9273\times10^{-20}$ erg/G; $a_0=0.5292\times10^{-8}$ cm and $\mathbf{r}$ is now given in atomic units. The terms in $\mathbf{H}_{\text{eff}}$ are the anisotropic and isotropic (contact) fields, respectively. To compute the average field due to N electrons within the single-determinant orthogonal-orbital model, one finds

$$\mathbf{H}_{\text{av}}=\sum_{i=1}^{N}\langle i\,|\,\mathbf{H}_{\text{eff}}\,|\,i\rangle. \tag{5.4}$$

A. Calculations and Results for the Ni_2F Cluster

Consider the triatomic cluster, Fig. 7, in which S and I are quantized along some external magnetic field $\mathbf{H}_0$. We may write out the energy expression explicitly in terms of the direction cosines $\cos\theta_\sigma$, $\cos\theta_\pi$, and $\cos\theta_\mu$ of $\mathbf{H}_0$ on the molecular axes:

$$W=\frac{g_e\beta}{a_0^3}\gamma_N\hbar I_N m_s\left(\frac{3x^2-r^2}{r^5}\cos^2\theta_\pi+\frac{3y^2-r^2}{r^5}\cos^2\theta_\mu+\frac{3z^2-r^2}{r^5}\cos^2\theta_\sigma-\frac{8\pi}{3}\delta(\mathbf{r})+\frac{6xy}{r^5}\cos\theta_\pi\cos\theta_\mu+\frac{6xz}{r^5}\cos\theta_\pi\cos\theta_\sigma+\frac{6yz}{r^5}\cos\theta_\mu\cos\theta_\sigma\right). \tag{5.5}$$

For comparison with experimental parameters we may use the relation $\cos^2\theta_\pi+\cos^2\theta_\mu+\cos^2\theta_\sigma=1$, and rewrite Eq. (5.5) as

$$W=\frac{g_e\beta}{a_0^3}\gamma_N\hbar I_N m_s\left(\frac{x^2-y^2}{r^5}(3\cos^2\theta_\pi-1)+\frac{z^2-y^2}{r^5}(3\cos^2\theta_\sigma-1)-\frac{8\pi}{3}\delta(\mathbf{r})+\frac{6xy}{r^5}\cos\theta_\pi\cos\theta_\mu+\frac{6xz}{r^5}\cos\theta_\pi\cos\theta_\sigma+\frac{6yz}{r^5}\cos\theta_\mu\cos\theta_\sigma\right). \tag{5.6}$$

In the usual parametric form, one writes

$$W=\mathbf{S}\cdot\mathbf{A}\cdot\mathbf{I}, \tag{5.7}$$

where $\mathbf{S}$ is taken to be the spin of a single metal ion interacting with the nucleus. It has been shown that the tensor $\mathbf{A}$ is diagonal for cubic systems,[26] and Eq.

TABLE V. SCF calculation for Ni^{2+}-F^--Ni^{2+} system without crystal field. Accuracy in E_{elec}, 0.001.

E_{elec} orbital	Ferromagnetic configuration −319.7683 energy α spin	β spin
$1a_{1g}$	−25.769	−25.766
$2a_{1g}$	−1.390	−1.303
$3a_{1g}$	−1.243	−1.177
$4a_{1g}$	0.149	0.187
$5a_{1g}$	1.434	•••
$1a_{1u}$	−4.865	−4.830
$2a_{1u}$	−3.326	−3.269
$3a_{1u}$	−1.640	−1.661
$4a_{1u}$	−0.465	•••
$1e_{1g}$	−0.401	−0.368
$2e_{1g}$	0.336	0.407
$3e_{1g}$	0.864	0.881
$1e_{1u}$	−0.740	−0.681
$2e_{1u}$	0.001	0.013
$1e_{2g}$-ϵ	0.563	•••
$1e_{2g}$-θ	0.581	0.596
$1e_{2u}$-ϵ	0.060	•••
$1e_{2u}$-θ	0.084	0.100

[25] A. Abragam, *Principles of Nuclear Magnetism* (Clarendon Press, Oxford, 1961), p. 172.

[26] W. Marshall and R. Stuart, Phys. Rev. **123**, 2048 (1961).

(5.7) can be written as

$$W=A_s\mathbf{S}\cdot\mathbf{I}+(A_\sigma+A_D)\sum_r S_rI_r(3\cos^2\theta_{r\sigma}-1)+A_\pi\sum_r S_rI_r(3\cos^2\theta_{r\pi}-1). \quad (5.8)$$

By comparing Eq. (5.8) with Eqs. (5.2), (5.4), and (5.6), we have the correspondence

$$A_s=\frac{g_e\beta\gamma_N\hbar}{a_0^3S}\sum_{i=1}^{N}\langle i\mid-(8\pi/3)m_s\delta(\mathbf{r})\mid i\rangle,$$

$$A_\sigma+A_D=\frac{g_e\beta\gamma_N\hbar}{a_0^3S}\sum_{i=1}^{N}\langle i\mid m_s[(z^2-y^2)/r^5]\mid i\rangle,$$

$$A_\pi=\frac{g_e\beta\gamma_N\hbar}{a_0^3S}\sum_{i=1}^{N}\langle i\mid m_s[(x^2-y^2)/r^5]\mid i\rangle. \quad (5.9)$$

Here S is the magnitude of the total electron spin of the system. We note that the additional terms contributing to Eq. (5.6) make no contribution to the energy due to their angular dependence. However, these terms may be important for systems with lower-than-cubic symmetry.

The orbitals used in these calculations are products of space and spin functions

$$\mid i\rangle=\Phi_i(\mathbf{r})\chi_i(s), \quad (5.10)$$

with $m_s=\pm\frac{1}{2}$. With the limited bases employed in our crude one-center expansion, the orbitals are also separable into radial and angular functions, the latter being real spherical harmonics:

$$\Phi_i(\mathbf{r})=N_iR_i(r)P_l^m(\theta)S_m^\sigma(\varphi). \quad (5.11)$$

The spin part of the matrix elements [Eq. (5.9)] is trivially obtained, and the angular integrals are easily evaluated by making use of the vector coupling coefficients for spherical harmonics.[27] The result may be written as

$$A_s=\frac{g_e\beta\gamma_N\hbar}{a_0^3S}\sum_{i=1}^{N}[-(8\pi/3)m_s\mid\Phi_i(0)\mid^2],$$

$$A_\sigma+A_D=\frac{g_e\beta\gamma_N\hbar}{a_0^3S}\sum_{i=1}^{N}m_s(A_{lm\sigma}+\tfrac{1}{6}B_{lm\sigma})\langle i\mid\mid 1/r^3\mid\mid i\rangle,$$

$$A_\pi=\frac{g_e\beta\gamma_N\hbar}{a_0^3S}\sum_{i=1}^{N}m_s(\tfrac{1}{3}B_{lm\sigma})\langle i\mid\mid 1/r^3\mid\mid i\rangle. \quad (5.12)$$

The angular coefficients are given by

$$A_{lm\sigma}=\int d\Omega\mid P_l^mS_m^\sigma\mid^2P_2^0\Big/\int d\Omega\mid P_l^mS_m^\sigma\mid^2,$$

$$B_{lm\sigma}=\int d\Omega\mid P_l^mS_m^\sigma\mid^2P_2^2S_2^0\Big/\int d\Omega\mid P_l^mS_m^\sigma\mid^2, \quad (5.13)$$

[27] See, for example, M. E. Rose, *Elementary Theory of Angular Momentum* (John Wiley & Sons, Inc., New York, 1957).

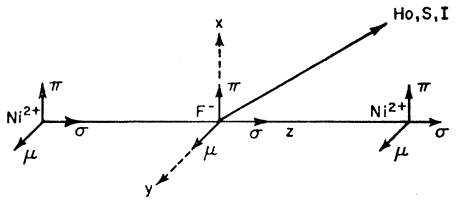

FIG. 7. $(NiF)^{3+}$ molecular geometry.

and a short list is given in Table VI. The formulas given reduce to those found by Marshall and Stuart[26] for MnF_2 using the "antibonding LCAO" independent bonding model. Our molecular-orbital–self-consistent-field (MO-SCF) treatment directly includes metal overlap onto the ligand, which had been previously omitted, as well as $1s$-$2s$ orthogonality (cross) terms in the contact interaction.[26,28]

The classical dipole term A_D may be extracted by assuming a spin density on each Ni^{2+} ion which does not overlap the fluorine site. In this $(3d)^8$ problem the nearly spin-paired orbitals make small contributions to the dipole field, which can be taken into A_σ, so we merely consider the $(e_g^\uparrow)^2$ unpaired orbitals. To evaluate A_D one must compute matrix elements of the interaction W [Eq. (5.6)] with orbitals $\mid 3z^2-r^2\rangle$ and $\mid x^2-y^2\rangle$ centered on a nickel ion. The resulting two-center integrals are evaluated using spherical-harmonic expansions of $P_2^mS_m^\sigma/r^3$ with the result that for a single ion

$$\tfrac{1}{2}A_D=\frac{g_e\beta\gamma_N\hbar}{2a_0^3S}\left(\frac{2}{R^3}+\frac{7\langle 3d\mid\mid r^4\mid\mid 3d\rangle}{R^7}\right), \quad (5.14)$$

where $\langle 3d\mid\mid r^4\mid\mid 3d\rangle$ is the reduced (radial) matrix element.

We now refer to the calculations on $(Ni_2F)^{3+}$, in which the Ni^{2+} core $(1s)^2(2s)^2(2p)^6$ has been treated as a point charge. Unlike the experimental situation, the remaining 42 electrons are assembled in an $S_z=2$ state corresponding to a half-filled e_g shell on each of the $(3d)^8$ metal ions. The symmetry orbitals and the number of occupied levels of either spin are listed in Table VII. Contributions to the isotropic contact field are limited to the a_{1g} orbitals; individual contributions to the spin density $\sum_i 2(m_s)_i\mid\Phi_i(0)\mid^2$ are shown in Table VIII. It appears that spin density arising from orbital pairs is largely self-canceling, and that the dominant term is the unpaired $5a_{1g}^\uparrow$ density. However, slight changes in this function will produce drastic variations in the contact spin density due to its F($1s$, $2s$) components. For this reason, one may not expect accurate results with a very limited basis set such as the one used here.

Another type of error is due to the cluster model itself; in the $KNiF_3$ crystal each Ni ion bonds with six neighboring ligands, and the present triatomic model

[28] A. J. Freeman and R. E. Watson, Phys. Rev. Letters **6**, 343 (1961).

TABLE VI. Angular coefficients for hyperfine interaction.

L	M	$A_{lm\sigma}$	$B_{lm\sigma}$
0	0	0	0
1	0	2/5	0
1	1	−1/5	$(-1)^{\sigma}6/5$
2	0	2/7	0
2	1	−8/35	$(-1)^{\sigma}6/7$
2	2	−16/35	0
3	0	4/15	0
3	1	−4/35	$(-1)^{\sigma}4/5$
3	2	−38/105	0
3	3	−10/21	0

will tend to overemphasize the bonding. The fact that the spin-polarized wave function is not an eigenstate of S^2 may also be a source of error; however, the deviation is small and experience with free-ion calculations[29] would indicate that the error introduced is also small.[30] The value of A_s found from Eq. (5.12) is

$$A_s = 517\times10^{-4}\ \text{cm}^{-1}$$

corresponding to a contact field

$$H^c = 774\ \text{kG}.$$

The experimental value[31] of A_s is 33.9×10^{-4} cm^{-1}.

We now consider the anisotropic hyperfine interaction. The required radial integrals are given in Table IX for each representation Γ and either spin. The tabulated integrals are sums over the matrix elements of $1/r^3$ for the occupied orbitals of each species:

$$\langle 1/r^3\rangle_\Gamma{}^{\uparrow} = \sum_{i\in\Gamma,\, m_s=1/2} \langle i \,||\, 1/r^3 \,||\, i\rangle.$$

TABLE VII. Symmetry orbitals for the $(Ni_2F)^{3+}$ cluster.

Symmetry	Participating ion orbitals	$n\uparrow$	$n\downarrow$	L	M
a_{1g}	F(1s, 2s) Ni(3s, 3pσ, 3dσ)	5	4	0	0
a_{1u}	F(2pσ) Ni(3s, 3pσ, 3dσ)	4	3	1	0
e_{1g}	F(2pπ) Ni(3pπ, 3dπ)	6	6	1	1
e_{1u}	Ni(3pπ, 3dπ)	4	4	2	1
e_{2g}	Ni(3dδ)	2	1	2	2
e_{2u}	Ni(3dδ)	2	1	3	2

TABLE VIII. $(Ni_2F)^{3+}$ contact spin density $\sum_i 2(m_s)_i \,|\, \Phi_i(0)\,|^2$.

Orbital	Spin density	
$1a_{1g}$	+0.192 a.u.	F(1s)+···
$2a_{1g}$	+1.424	F(2s)+Ni(3s)+···
$3a_{1g}$	−1.480	Ni(3s)+F(2s)+···
$4a_{1g}$	+0.024	Ni(3pσ)+Ni(3dσ)+···
$5a_{1g}$	+1.316	Ni(3dσ)+Ni(3pσ) +F(2s)+F(1s)+···
total a_{1g}	+1.476	

Because of cylindrical symmetry the effective field

$$H^{\pi} = (g_e\beta/2a_0^3)\sum_\Gamma \tfrac{1}{3}B_{lm\sigma}(\langle 1/r^3\rangle_\Gamma{}^{\uparrow} - \langle 1/r^3\rangle_\Gamma{}^{\downarrow}) \quad (5.15)$$

and the hyperfine parameter

$$A_\pi = H^{\pi}\gamma_N\hbar/S \quad (5.16)$$

are both zero. The two self-canceling components of H^{π} caused by spin unpairing in e_{1g} are $\pm0.042(g_e\beta/2a_0^3)$ in magnitude and the components of the e_{1u} representation are negligible.

The nonzero components of

$$H^{\sigma} = (g_e\beta/2a_0^3)\sum_\Gamma (A_{lm\sigma}+\tfrac{1}{6}B_{lm\sigma})(\langle 1/r^3\rangle_\Gamma{}^{\uparrow} - \langle 1/r^3\rangle_\Gamma{}^{\downarrow}) \quad (5.17)$$

are given (in units $g_e\beta/2a_0^3$) in Table X, with the results

$$H^{\sigma} = +19.33\ \text{kG},$$

$$A_\sigma + A_D = H^{\sigma}\gamma_N\hbar/S = 12.91\times10^{-4}\ \text{cm}^{-1}.$$

From Eq. (5.14) and the calculated value[29] of $\langle r^4\rangle_{3d}=3.0034$, we obtain values of the dipole field H^D and the parameter A_D as

$$H^D = -4.82\ \text{kG},$$

$$A_D = -3.22\times10^{-4}\ \text{cm}^{-1}.$$

The dipole field from the rest of the crystal has been

TABLE IX. Radial integrals $\langle 1/r^3\rangle_\Gamma$ in $(a_0)^{-3}$ units and $R=3.79271a_0$.

Symmetry	Spin ↑	Spin ↓
a_{1u}	5.705	6.538
e_{1g}-ε	9.141	9.246
e_{1g}-θ	9.141	9.246
e_{1u}-ε	0.061	0.061
e_{1u}-θ	0.061	0.061
e_{2g}-ε	0.023	···
e_{2g}-θ	0.023	0.023
e_{2u}-ε	0.020	···
e_{2u}-θ	0.020	0.020
$F^-\langle 1/r^3\rangle_{2p}$	6.405	6.405[a]
R^{-3}	0.01832	

[a] C. Froese, Proc. Camb. Phil. Soc. **53**, 206 (1957).

[29] A. J. Freeman and R. E. Watson, in *Magnetism*, edited by G. Rado and H. Suhl (Academic Press Inc., New York, 1965), Vol. IIA, p. 167.

[30] As we have noted previously, the single-determinant wave function is not an eigenstate of S^2. While one may calculate properties which depend upon the spin density, the results must be viewed with some caution. The deviation of $\langle S^2\rangle$ from the eigenvalue $S(S+1)$ (measured essentially by $\Sigma_\beta(-\Sigma_\alpha S_{\alpha\beta}{}^2)$, where $S_{\alpha\beta}$ are the overlap integrals between orbitals of opposite spin in all shells) is usually quite small, <1%, for these clusters. However, one would prefer to treat the spin problem within the HF scheme using either a variational constraint or spin-projected determinants; cf. F. E. Harris, J. Chem. Phys. **46**, 2769 (1967).

[31] R. G. Shulman and S. Sugano, Phys. Rev. **130**, 506 (1963).

omitted, and so the calculated value of A_σ is

$$A_\sigma = +16.13\times10^{-4}\ \text{cm}^{-1},$$

to be compared with the experimental value[31] 8.8×10^{-4} cm^{-1}. Thus, unlike the results obtained for A_s, there is order-of-magnitude agreement with experiment for A_σ.

B. Results for the NiF_6 Cluster

We describe briefly the results obtained for the NiF_6 cluster both for completeness and in order to point out the crude ligand spin densities obtained with these limited one-center basis functions.

The spin density at an F^- site was computed from the ground-state cluster wave function, which was first orthogonalized to the F^- 1s orbitals, as

$$\rho^s = \rho^s(a_{1g}) + \rho^s(e_g) + \rho^s(t_{1u}), \tag{5.18}$$

where

$$\rho^s(\Gamma) = \sum_{i\varepsilon\Gamma} 2(m_s)_i \,|\, \psi_i(\mathbf{r}) \,|^2_{r=(00R)}$$

is the contribution of all orbitals of symmetry Γ. From ρ^s we may easily calculate A_s as defined by Eq. (5.12).

In the usual LCAO picture a variety of corrections[26,28] are applied to obtain ρ^s, because of the nonorthogonality of orbitals used to describe the cluster. In our calculations, all of these effects are included automatically and one merely adds up the spin densities of all orbitals. The spin density ρ^s and fractional density f_s computed in this way for $(NiF_6)^{4-}$ was found to be an order of magnitude smaller than the experimentally obtained value.[31] As already emphasized, this result was to be expected since our limited basis does not have sufficient *angular* freedom to build up a large ligand density at the F^- sites, although the radial behavior is quite good. It is worth noting that while the dominant contribution to f_s comes from the unpaired $3e_g$ α orbital, the *sum* of contributions from the spin-split orbitals of the a_{1g} (s-like), t_{1u} (p-like), and e_g (d-like) representations is of nearly equal magnitude.

VI. BONDING EFFECTS AND NEUTRON DIFFRACTION

The effects of covalency on the measured neutron magnetic scattering from magnetic salts have recently been considered by Hubbard and Marshall[32] (HM). Using a simple one-electron antibonding LCAO wave function and covalency parameters determined empirically, these authors have shown that covalent bonding affects both the absolute intensities and form factors in a significant way. Here we calculate the neutron-magnetic form factors from the cluster MO's discussed earlier. Our form-factor results confirm those obtained more simply by HM and show quantitatively some of the effects discussed qualitatively by them.

TABLE X. Contributions to H^σ by symmetry representation.

Representation	H_σ
a_{1u}	−0.3332
e_{1g}-θ	0.0420
e_{2g}-ϵ	−0.0105
e_{2u}-ϵ	−0.0072
total	−0.3089

The magnetic form factor describing the coherent scattering of neutrons by the magnetization density is given by

$$f(\mathbf{K}) = \int dv\, \rho(r)\, \exp(i\mathbf{K}\cdot\mathbf{r}), \tag{6.1}$$

where $\mathbf{K}$ is the scattering vector [with $|\mathbf{K}| = 4\pi(\sin\theta)/\lambda$, where θ is the scattering angle and λ the neutron wavelength], and $\rho(r)$ is the electron spin density surrounding each one of an equivalent set of magnetic ions in the crystal. Using the expansion

$$\exp(i\mathbf{K}\cdot\mathbf{r}) = 4\pi\sum_l i^l(2l+1)j_l(Kr)P_l(\theta_{12}), \tag{6.2}$$

where $j_l(Kr)$ is the lth spherical Bessel function, Eq. (6.1) is simply evaluated as

$$f(\mathbf{K}) = \sum C_{lm} f_{lm}(K)\, Y_{lm}(\Omega_K). \tag{6.3}$$

The coefficients C_{lm} are factors and angular integrals of products of spherical harmonics easily evaluated in terms of the vector coupling coefficients. The radial integrals

$$f_{lm}(K) = \int r^2 dr\, \rho_{lm}(K) j_l(Kr) \tag{6.4}$$

may be further divided into contributions from each representation, since

$$\rho_{lm} = \sum_\Gamma \rho_{lm}{}^\Gamma.$$

We have computed the functions $f_l(K)$ for $l=0$ and 4, which are the leading nonzero terms for a cubic complex, for each spin in each representation of the $(NiF_6)^{4-}$ cluster. We find that the neutron scattering is dominated by the open e_g shell; the contributions from other symmetries due to spin polarization are only 1 or 2% of the e_g term. The corresponding calculations have been made for the Ni^{2+} ion computed in the $KNiF_3$ crystal field in order to provide a comparison between the single-ion and cluster spin densities.

The $f_0(K)$ contribution is the well-known spherical ($l=0$) term in the form factor while the $f_4(K)$ contributes experimentally substantial deviations ("bumps") from the smooth spherical form factor.[33] Figure 8 compares the $f_4(K)$ terms calculated for the Ni^{2+} ion in the $KNiF_3$ crystal field with the computed $(NiF_6)^{4-}$-complex spin density. While both show the usual peaking at large angles, the covalent spin density

[32] J. Hubbard and W. Marshall, Proc. Phys. Soc. **86**, 561 (1965).

[33] A. J. Freeman, Acta Cryst. **12**, 261 (1959); R. J. Weiss and A. J. Freeman, J. Phys. Chem. Solids **10**, 147 (1959).

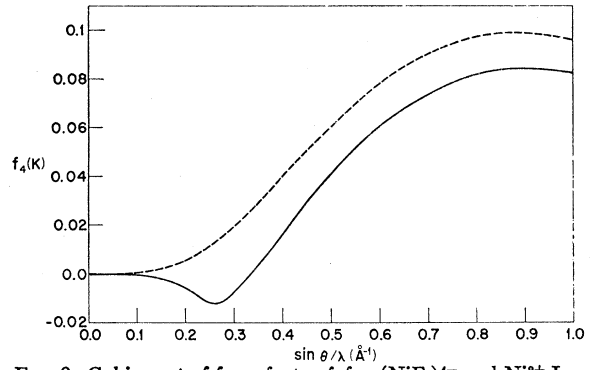

FIG. 8. Cubic part of form factor f_4 for $(NiF_6)^{4-}$ and Ni^{2+} Ion.

shows an unusual negative dip at low angles at which some important reflections occur. The dip is a manifestation of bonding effects, here manifested on the nonspherical (cubic) part of the magnetic form factor.

More striking is the effect of covalency on the $f_0(K)$ form factor. Figure 9 compares the single-ion and cluster $f_0(K)$ form factors, both shown normalized to 1 at $(\sin\theta)/\lambda=0$. The large differences observed at low scattering angles reflect the obvious fact that the spin density of the cluster has a significant contribution which resides on the ligand sites.

An even more dramatic way of showing the effect of this ligand (covalent) spin density is to renormalize[32] the free-ion $f(\mathbf{K})$ curve in order to allow for the reduction in absolute intensity observed in neutron measurements. Using the same scale factor (0.82) employed by HM, we show such a comparison in Fig. 10. Here the peak in the forward scattering direction[32] is clearly seen, along with some additional structure at somewhat larger angles. This additional structure does not appear in the antiferromagnetic case[34] because there is an exact cancellation of the spin density at the ligand site

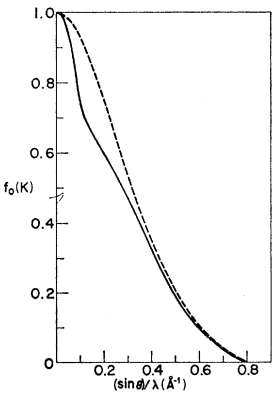

FIG. 9. Spherical part of the form factor f_0 for $(NiF_6)^{4-}$ and the Ni^{2+} ion in an external field.

which does not occur in the ferromagnetic (or paramagnetic) case, and it is this ligand density which is responsible for the structure (barely visible) at $(\sin\theta)/\lambda\approx 0.2$ in Fig. 10.

Since the cluster calculations reported in this paper suffer from a number of approximations (discussed earlier), we shall not compare in detail our calculated values with experimental data, such as Alperin's[35] on NiO. (To our knowledge $KNiF_3$ has not been investigated.) We find that our computed $f(\mathbf{K})$ lies below the experimental data even when the latter is scaled by the factor 0.82. It does, however, lie above the free-ion curve (as is evident from Fig. 10). Part of the improvement over the free-ion value is due to the allowance for spin polarization (first considered for Ni^{2+} by Watson and Freeman[36]), an allowance carried through, however, for the calculated $f(\mathbf{K})$ curves shown in Figs. 8–10. While the inclusion of the scattering from the unquenched orbital moment of the Ni^{2+} ion, discussed by Blume,[37] would also help the agreement with experiment, the final neutron form factor is still too small at scattering values $>0.4A^{-1}$.

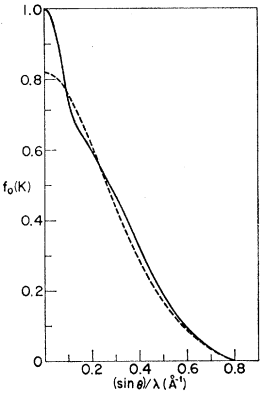

FIG. 10. Spherical part of the form factor f_0 for $(NiF_6)^{4-}$ and Ni^{2+} ion (scaled to 0.82).

More accurate cluster calculations would, of course, be of interest for the Ni^{2+} systems. However, calculations for the Mn^{2+} complexes would be of perhaps greater interest since these show a form factor which lies well *below* the free-ion values and show no reduction in absolute intensity in the forward direction, as emphasized by HM. Neither of these effects is understood presently using simplified LCAO models. More rigorous calculations are in progress and results will be reported in the near future.[38]

VII. DISCUSSION OF RESULTS AND CONCLUSION

The calculations on Ni^{2+}, $Ni^{2+}F_6^-$, and $Ni_2^{2+}F^-$ clusters reported in this paper emphasize the importance

[34] It should, however, be emphasized that we are describing our results for an isolated NiF_6 cluster for which there is no cancellation of the spin density on the ligand sites, as is the case for antiferromagnetic ordering. The comparisons are made here to the antiferromagnetic case because only for very small scattering angles [where our $f(\mathbf{K})$ curve has a sharp peak] would the two differ significantly, and because experimental data are available only for the antiferromagnetic case.

[35] H. A. Alperin, Phys. Rev. Letters **6**, 55 (1961).

[36] R. E. Watson and A. J. Freeman, Phys. Rev. **120**, 1125 (1960); **120**, 1134 (1960).

[37] M. Blume, Phys. Rev. **124**, 96 (1961).

[38] D. E. Ellis and A. J. Freeman, Bull. Am. Phys. Soc. **13**, 482 (1968).

of treating all electrons of these molecular clusters in a self-consistent manner. We accomplished this by generating symmetry orbitals for the clusters which may be any variationally determined mixture of central-ion and ligand basis functions.

At this point we should emphasize once more that our results, though they are self-consistent, still are a very crude approximation to a solution of the Hartree-Fock equations. This is mainly due to the limited character of our basis set which, at this level of effort, is probably inferior to a minimal Slater basis. It is very well possible that the crude basis we are using affects some of the results (for instance, the ordering of the e_g, α orbitals). Although our calculations are not more than a very simple approach to more extensive HF calculations on these systems, they already indicate a number of features not found in earlier work. In particular, the spin splitting due to the open e_g shell is found to play a predominant role.

Our results show that in addition to the mixing of metal $3d$ and ligand orbitals usually considered in an LCAO-MO treatment there is a significant mixing in representations containing the metal $3s$ and $3p$ orbitals. Thus the covalency found in the a_{1g} and t_{1u} representations of NiF_6 seems as important as that of the e_g and t_{2g} symmetries in any LCAO picture of the system. The LCAO interpretation is further complicated by the necessity of describing the strong s-p ligand hybridization which is found; however, it serves as an invaluable qualitative guide in the choice of basis functions and in examining the self-consistent cluster orbitals. The fact that the orbitals which we have plotted can be clearly identified in terms of LCAO's of about the shape and energy ordering to be expected is satisfying, considering the very limited basis sets which were used.

It appears that the LCAO picture can be carried only so far in describing the molecular orbitals of these complexes since it has been known for a long time from studies on small molecules that free-atom orbitals form a rather poorly convergent basis set. For example, the $3s$ and $3p$ functions used here are not atomic metal orbitals but merely basis functions for our calculation. We know that a larger basis will give a more accurate wave function and may reduce the $3s$-$3p$–ligand mixing along with the $3d$-ligand mixing. However, we observe that *compared with* the $3d$ mixing, the $3s$-$3p$ mixing is still important and must be taken into account.

An alternative approach for the calculation of wave functions for transition-metal complexes which has received recent attention[1,6,26] is the familiar Heitler-London or so-called "configuration interaction" technique mentioned in the Introduction. The term "configuration interaction" is used advisedly because of very special assumptions made concerning the participating determinantal states. In this approach the interaction of metal and ligands in the cluster is considered as a perturbation on various free-ion states with a number of possible single-electron transfers taken into account. Thus for NiF_6 one might write the cluster wave function as a sum of states, each of which is taken to be the antisymmetrized product of free-ion states with particular orbital assignments for each ion.[6] The states which are expected to be important for NiF_6 would then include, for example, $Ni(3d^8)\times F(2s^2 2p^6)$, $Ni(3d^8 4s^1)\times F(2s^1 2p^6)$, $Ni(3d^9)\times F(2s^2, 2p^5)$, etc. [note that $F(2s^m 2p^n)$ actually means the proper combination of all six ligands]. The proponents of this method conclude that a correct description of the cluster must include electron-transfer effects of this type which involve excited states of the ions.

We may suggest that the MO-SCF single determinant method which is applied in the present work is capable of reproducing many of the effects described as one-electron transfers in the Heitler-London theory. The reason is simply that one is not bound to the restricted LCAO basis set and basis sets may be chosen which have sufficient variational freedom to permit an admixture of such functions as the metal $4s$ and $4p$ orbitals in the occupied molecular orbitals. The model calculations which we have made on $KNiF_3$ are not intended to be highly accurate MO solutions for the cluster problem, but were chosen instead to demonstrate the feasibility of the method and to reveal general features of the solution for a system of current interest. A strict comparison of the Heitler-London and MO-SCF results is not possible, because of the semiempirical nature of the H-L calculations to date; however, our results are sufficiently encouraging to conclude that the MO-SCF method merits further study.

The calculation of the crystal-field splitting for the Ni^{2+} and NiF_6 clusters reported here shows the necessity of taking into account the metal-ligand mixing of orbitals. Although the splitting between the ground and first excited states of NiF_6 is found to be of the right order of magnitude, one must be wary of attaching any great significance to the result. We see that the energy difference appears in the sixth significant figure of the total-cluster energies, and results from the detailed rearrangement of a large number of orbitals. The fond hope that the excitation energy could be treated simply as the promotion of a single electron from a t_{2g} to an e_g orbital without further rearrangement seems to be unjustified; this is the same conclusion reached in an earlier LCAO-MO study.[19] The very small role which the crystal field of ions external to NiF_6 plays in determining Δ may help to explain why the optical spectra are not very different for the complex in solution or in the crystal. We have already mentioned that the small size of crystal-field matrix elements results from the cancellation of regions in the vicinity of the ligands where the potential is large but varies in sign. In this connection one would like to extend these calculations to a basis with greater angular freedom to see to what extent this cancellation holds for more accurate wave functions.

The use of a spin-unrestricted wave function leads to

a reasonable splitting Δ; the pseudo-closed-shell wave function is useless for this purpose, since errors inherent to the pseudo-closed-shell estimation of Coulomb and exchange potentials are an order of magnitude greater than the splitting. The fact that a single-determinant wave function can lead to a reasonable value of Δ for NiF_6 (although it gives a poor F^- spin density for Ni_2F) is encouraging; however, we have no idea as yet what effect a spin projection of the wave function might have on these parameters.

Three major problems remain for future work. The first is to determine better single-determinant wave functions, and this requires considerable work to improve the type and number of basis functions used. The second problem is to discover those limited-configuration techniques which will allow a satisfactory description of the spin and will include significant correlation effects. The third, and perhaps most interesting, task is to carry out the complete self-consistent crystal solution which will (in the one-electron picture) lead eventually to the true Wannier orbitals of the system. Further work on these problems is in progress.

APPENDIX A: COMPUTATIONAL TECHNIQUES FOR THE MIXED ONE-CENTER BASIS SET

We first describe a method for computing function values for the function $\eta_{nlm;\lambda}(\alpha, r, R)$. This function can be written in terms of modified Coulson-Barnett ζ functions[39] according to

$$\eta_{nlm;\lambda}(\alpha, r, R) = \alpha^{-n+1}\frac{(\lambda-m)!}{(\lambda+m)!} \times \exp(-|\alpha r-\alpha R|)\sum_{i=m}^{l}\binom{l+m}{i+m}(\alpha R)^{l-i} \times(\alpha r)^{i}(-1)^{i+m}\sum_{j=|\lambda-i|}^{\lambda+i} D_j(\lambda m \mid im)\zeta_{n-l,j}(\alpha r, \alpha R). \quad \text{(A1)}$$

Here the coefficients D_j are the well-known vector coupling coefficients for spherical harmonics.[40] To compute ζ functions one may use the recursion formula

$$\zeta_{m+2,n} = (t^2+\tau^2)\zeta_{m,n} -[2t\tau/(2n+1)][n\zeta_{m,n-1}+(n+1)\zeta_{m,n+1}]. \quad \text{(A2)}$$

Starting values are given by

$$\zeta_{0,n}(t, \tau) = (t\tau)^{-1/2}\exp(r_>-r_<)I_{n+1/2}(r_<)K_{n+1/2}(r_>) \quad \text{(A3)}$$

and

$$\zeta_{1,n} = [t\tau/(2n+1)](\zeta_{0,n-1}-\zeta_{0,n+1}), \quad \text{(A4)}$$

where

$$r_< = (t, \tau)_<, \qquad r_> = (t, \tau)_>,$$

and $I_{n+1/2}$ and $K_{n+1/2}$ are modified Bessel functions.[41] A more complete discussion of ζ functions can be found in the literature.[42] The radial parts of some typical a and b functions are shown in Fig. 11.

The computation of one-electron integrals containing b-type functions is performed by straightforward numerical integration, using Gauss-Legendre quadrature points for the region between 0 and R and Gauss-Laguerre points for the region from R to ∞. The only trouble for the one-electron integrals may arise from the operators $-\frac{1}{2}\nabla^2$ (kinetic energy) and $\sum_B 1/r_B$ (interaction with ligand nuclei). For the kinetic energy one can derive that for $n>l$

$$-\tfrac{1}{2}\nabla^2 b_{nlm;\lambda\mu\sigma} = \tfrac{1}{2}\{[l(l+1)-n(n-1)]b_{n-2,lm;\lambda\mu\sigma} +2\alpha n b_{n-1,lm;\lambda\mu\sigma}-\alpha^2 b_{nlm,\lambda\mu\sigma}\}. \quad \text{(A5)}$$

Special formulas can be written for the case $n=l$. In order to obtain a formula for the $\sum_B 1/r_B$ operator one can expand $1/r_B$ for each ligand in a spherical-harmonic series about the central ion and then rotate all spherical harmonics to a common coordinate system. This leads to the expression

$$\sum_B r_B^{-1} = \sum_l \delta^l(r, R)\sum_{m,\sigma}\tfrac{1}{2}\epsilon_m[(l-m)!/(l+m)!] \times C(l, m, \sigma)P_l^m(\theta)S_m^\sigma(\varphi), \quad \text{(A6)}$$

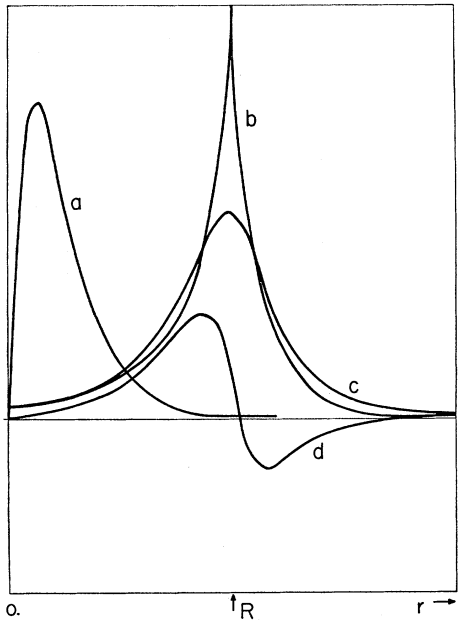

FIG. 11. Radial functions for the one-center basis. (a) $r^n e^{-\alpha r}$; (b) $\eta_{000,0}$; (c) $\eta_{100,0}$; (d) $\eta_{210,1}$.

[39] M. P. Barnett and C. A. Coulson, Phil. Trans. Roy. Soc. A243, 221 (1951).

[40] F. J. Corbato and A. C. Switendick, *Methods in Computational Physics*, edited by B. Adler, S. Fernbach, and M. Rotenberg (Academic Press Inc., New York, 1963). Vol. 2, p. 155.

[41] G. N. Watson, *Theory of Bessel Functions* (Cambridge University Press, New York, 1923).

[42] M. P. Barnett, *Methods in Computational Physics*, edited by B. Adler, S. Fernbach, and M. Rotenberg (Academic Press Inc., New York, 1963). Vol. 2, p. 95.

where

$$\delta^l(r, R) = r_<^l / r_>^{l+1},$$

$$\epsilon_m = 1 \quad \text{for} \quad m = 0, \qquad \epsilon_m = 2 \quad \text{for} \quad m \neq 0,$$

$$C(l, m, \sigma) = \sum_B D_{0m}^{l0\sigma}(\alpha_B, \beta_B, \gamma_B).$$

The coefficients D are rotation coefficients for spherical harmonics[43] and α_B, β_B, γ_B are rotation angles corresponding to the ligand B. For the two-electron integral

$$I = \int dv_1 \Phi_i^*(\mathbf{r}_1) \Phi_j(\mathbf{r}_1) \int dv_2 \Phi_k^*(\mathbf{r}_2) \Phi_l(\mathbf{r}_2) r_{12}^{-1} \quad \text{(A7)}$$

the operator $1/r_{12}$ is expanded in spherical harmonics about the central ion and the integral then can be written as a finite sum of products of radial and angular integrals

$$I = \sum_l R(l) A(l). \quad \text{(A8)}$$

The angular integrals $A(l)$ are easily computed with the help of orthogonality relations for spherical harmonics. The radial integrals are

$$R(l) = \int_0^\infty dr_1 \rho_1(r_1) \int_0^\infty dr_2 \rho_2(r_2) \delta^l(r_1, r_2), \quad \text{(A9)}$$

where $\rho_1(r_1)$ is the radial part of $r_1^2 \Phi_i^* \Phi_j$ and $\rho_2(r_2)$ is the radial part of $r_2^2 \Phi_k^* \Phi_l$. After partial integration, Eq. (A9) may be expressed as

$$R(l) = (2l+1) R \left\{ \int_0^1 dt \left[\int_0^1 \rho_1(utR) u^l du \right] \times \left[\int_0^1 \rho_2(utR) u^l du \right] + \int_0^1 (dt/t^2) \left[\int_0^1 \rho_1(uR/t) u^l du \right] \times \left[\int_0^1 \rho_2(uR/t) u^l du \right] \right\}. \quad \text{(A10)}$$

Using this integral transformation an efficient scheme for computing two-electron integrals may be obtained as follows:

(1) Compute first a two-dimensional grid of integration points using the Gauss-Legendre method.

(2) Compute the radial-function values of all basis functions Φ_j at all points.

(3) With these function values, compute intermediate integrals of the type

$$\int_0^1 \rho(utR) u^l du \quad \text{and} \quad (1/t) \int_0^1 \rho(uR/t) u^l du$$

for all possible charge densities ρ.

(4) In order to compute a two-electron integral, now first compute the angular integrals $A(l)$. If these integrals are nonzero, construct the radial integrals $R(l)$ from the intermediate integrals and sum over l. Using this approach, two-electron integrals were computed on an IBM 7094 computer with an accuracy of at least 10^{-6} a.u. and with typical computation times of 1–5 msec.

The computation of two-electron integrals is also speeded up by the fact that we can take advantage of cases where all degenerate components of a given symmetry species are occupied in the molecular wave function. The secular equations for each component are identical and there is no necessity of carrying about redundant information; therefore, when two-electron integrals are computed, all degenerate components are immediately summed into the Coulomb and exchange potentials. As an example, consider the interaction of function pair (i, j) with the fully occupied triplet of functions $t_{2g}(\xi, \eta, \zeta)$; the integrals which are actually computed are

$$V_{i,j}^{\text{Coul}}(t_{2g}) = \langle ij \mid 1/r_{12} \mid \xi\xi + \eta\eta + \zeta\zeta \rangle,$$

$$V_{i,j}^{\text{Exch}}(t_{2g}) = \langle i\xi \mid 1/r_{12} \mid j\xi \rangle + \langle i\eta \mid 1/r_{12} \mid j\eta \rangle + \langle i\zeta \mid 1/r_{12} \mid j\zeta \rangle. \quad \text{(A11)}$$

In this way redundancy in the computation of radial integrals is eliminated and the number of integrals which must be manipulated is greatly reduced.

APPENDIX B: CRYSTAL-FIELD POTENTIAL AND MATRIX ELEMENTS FOR A ONE-CENTER BASIS SET

1. Coulomb Field

The crystal-field potential may be written as

$$V(\mathbf{r}) = \sum_{LM\Sigma} V_{LM\Sigma}(r) P_L^M(\mu) S_M^\Sigma(\varphi) \tfrac{1}{2}\epsilon_M \frac{(L-M)!}{(L+M)!} \quad \text{(B1)}$$

expanded about the central ion. For cubic crystals we have the selection rules

$$\Sigma = 0,$$

$$L = 0, 4, 6, 8, \cdots,$$

$$M = 0, 4, 8, \cdots, L.$$

For a one-center basis set having maximum orbital momentum $l_{\max}$, the only nonzero matrix elements are for $L \leq 2l_{\max}$. We do not compute the $L=0$ (Madelung) term directly, but compute deviations from the (constant) Madelung potential. If the Madelung constant is known, the matrix elements can be placed on an absolute scale, and are computed in atomic units (a.u.).

The radial function $V_{LM\Sigma}$ may be written

$$V_{LM\Sigma}(r) = \sum_\nu C_{LM\Sigma}(\nu) U_{\nu L}(r), \quad \text{(B2)}$$

where the sum is over all ion shells exterior to the cluster. $C_{LM\Sigma}(\nu)$ is a coefficient obtained by summing rotation elements for all ions of a shell. If the basis orbi-

[43] J. O. Hirschfelder, C. F. Curtiss, and B. B. Bird, *Molecular Theory of Gases and Liquids* (John Wiley & Sons, Inc., New York, 1954), p. 905.

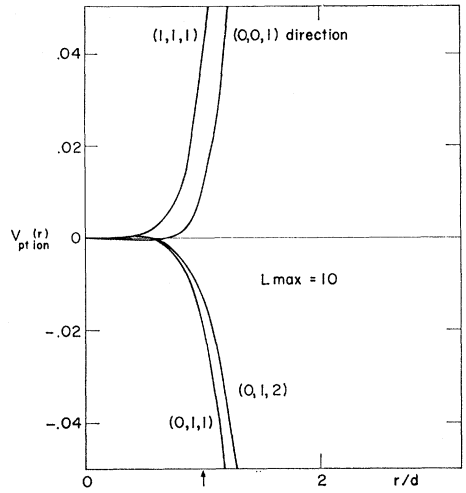

FIG. 12. Point-ion potential for $(NiF_6)^{4-}$ in $KNiF_3$.

tals are of the form $\Phi_{nlm\sigma}(\mathbf{r})=NR_{nl}(r)P_l^m(\mu)S_m^\sigma(\varphi)$, the matrix elements appear as

$$\langle\Phi\mid V(\mathbf{r})\mid\Phi'\rangle=\tfrac{1}{2}(2\pi NN')\delta_{\sigma'\sigma}\sum_{L,M,\pm}\frac{S(\pm)}{(2L+1)}\times D_L(l,m\mid l',\mp m')\delta_{|m\pm m'|,M}\mathrm{RAD}_{LM,nl,n'l'}. \quad \text{(B3)}$$

For $\Sigma=0$, the sign functions are $S(+)=(-1)^\sigma$, $S(-)=+1$. The D_L are vector coupling coefficients, and since L is even, we have $l+l'$ even for nonzero elements. The radial integral is

$$\mathrm{RAD}_{LM,nl,n'l'}=\int_0^\infty r^2drR_{nl}(r)R_{n'l'}(r)V_{LM0}(r). \quad \text{(B4)}$$

To compute the radial integrals we divide the sum ν over shells of ions into a "near-field" and a "far-field" part:

$$V_{LM\Sigma}(r)=\sum_{\nu=1}^{\mu}C_{LM\Sigma}(\nu)U_{\nu L}(r)+\left(\sum_{\nu=\mu+1}^{\nu_{\max}}C_{LM\Sigma}(\nu)\frac{Z_\nu r^L}{R_\nu^{L+1}}\right). \quad \text{(B5)}$$

The far-field or outer-shells sum is given in the non-overlapping point-ion approximation. The near-field or inner-shells sum takes all overlap effects into account.

The parameters μ and $\nu_{\max}$ can be chosen to obtain any required accuracy in the matrix elements. Since $R_\nu=(n_x^2(\nu)+n_y^2(\nu)+n_z^2(\nu))^{1/2}d$, where d is half of the cube edge, we may rewrite the far-field sum as

$$\left(\sum_{\nu=\mu+1}^{\nu_{\max}}C_{LM\Sigma}(\nu)\frac{Z_{\mathrm{eff}}(\nu)}{n_\nu^{(L+1)/2}}\right)\frac{r^L}{d^{L+1}}=C_{LM\Sigma}'\frac{r^L}{d^{L+1}}.$$

Thus

$$V_{LM\Sigma}(r)=C_{LM\Sigma}'\frac{r^L}{d^{L+1}}+\sum_{\nu=1}^{\mu}C_{LM\Sigma}(\nu)U_{\nu L}(r). \quad \text{(B6)}$$

We may now consider the radial potential $U_{\nu L}$ in the case of a spherically symmetric screening charge density. The charge density may be represented by a superposition of Slater orbitals. In that case,

$$U_{\nu L}(r)=Z_{\mathrm{eff}}(\nu)\delta_L(r,R_\nu)-\sum_{i,j}S_{ij}\frac{4\pi D_iD_j}{\alpha_{ij}{}^{n_{ij}}}\times(2L+1)\sum_{K=0}^{\lambda}\frac{\lambda!(\lambda-K+1)}{K!}\bar{\xi}_{K,L}(\alpha r,\alpha R), \quad \text{(B7)}$$

where

$Z_{\mathrm{eff}}(\nu)$ = net charge on ion;

S_{ij} = density coefficient for orbital pair i,j;

D_i, D_j = normalization constants for orbitals i,j;

$\alpha_{ij}=\alpha_i+\alpha_j$, α_i = orbital screening constant;

$n_{ij}=n_i+n_j$ (n_i = principal quantum number);

$\lambda=n_{ij}-1$;

$\bar{\xi}_{K,L}$ = molecular zeta function (modified).

The first term accounts for the overlap of cluster basis functions with a point ion, and the last is a correction for overlap of cluster and ion charge densities.

As mentioned before, only deviations from the Madelung ($L=0$) potential are computed. This means that the term $C_{000}(1/d)$ is omitted in Eq. (B6) and that $U_{\nu,0}$ is modified by replacing $\delta_0(r,R_\nu)$ by $\delta_0(r,R_\nu)-1/R_\nu$ in Eq. (B7).

By way of illustration we show in Fig. 12 the point-ion potential in several directions about a Ni^{2+} site in $KNiF_3$ including all ion shells from $(n1, n2, n3)=(1, 1, 1)$ to $(20, 20, 20)$ and truncated at an angular momentum $L=10$. Extending the sum to higher L acts to make the walls of the potential somewhat steeper as one approaches the edge of the cavity. In Fig. 13 we plot the $L=4$ component of the point-ion potential separately. Since very restricted basis sets will only sample small-L components of the potential, one obtains a very different picture of the crystal environment. We

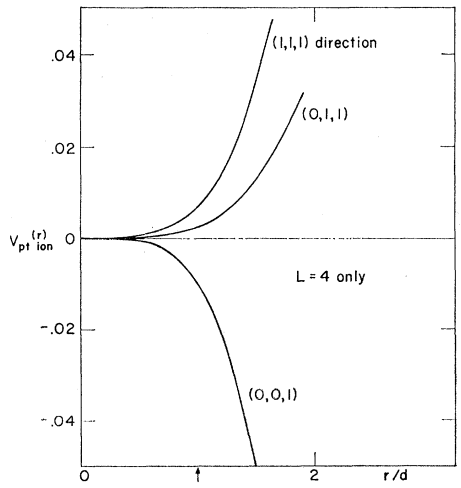

FIG. 13. $L=4$ component of point-ion potential.

may note that the $L=4$ component even shows the opposite sign to the total potential beyond the ligand (F^-) radius in the (001) and (011) directions. In view of our limited basis set calculations, this leaves the size of the actual external crystal-field splitting somewhat questionable.

As an example of the size and importance of overlap corrections to the point-ion potential we plot in Fig. 14 the overlap correction for the $(F^-)_6$ ligand shell. The quantity plotted is $C_{L00}U_L(r)$ with $Z_{\text{eff}}=0$ in Eq. (B6), using Clementi's F^- wave function.[13] Since the overlap correction decays exponentially with r, only the first few shells of neighbors need be included in the overlap sum.

2. Exchange Field

The simplest approach to the crystal exchange field is to consider first the two-center exchange integral

$$\langle AB \mid AB\rangle = \iint dv_1 dv_2 a_1^*(A,1) \times a_2(B,1)(1/r_{12})a_3^*(A,2)a_4(B,2). \quad \text{(B8)}$$

In particular let $a_2=a_4$, and write these functions as

$$a_i(B) = R_{nl}(r)\,Y_{lm}^{\sigma}(\theta,\varphi) \quad \text{(B9)}$$

in terms of normalized angular and radial functions. If the orbitals a_2 and a_4 are members of a fully occupied orbital shell, we may make use of the addition theorem:

$$\sum_{m,\sigma} Y_{lm}^{\sigma}(B,1)\,Y_{lm}^{\sigma}(B,2) = [(2l+1)/4\pi]P_l^0(B;1,2). \quad \text{(B10)}$$

Thus we shall treat *sums* of integrals of the $\langle AB \mid AB\rangle$ type over orbital closed shells on center B. Define the two-electron density for angular momentum L as

$$\rho_L(B;1,2) = \sum_i^{\text{shells } l=L} a_i^*(B,1)a_i(B,2), \quad \text{(B11)}$$

where, for example, ρ_0 is the summed two-particle density for electron $1s$, $2s$, $3s$, $\cdots$ shells. Using Eq. (B11), this can be written as

$$\rho_L(B;1,2) = [(2L+1)/4\pi]P_L^0(B;1,2) \times \sum_n^{\text{shells } l=L} R_{nl}(1)R_{nl}(2)$$
$$= [(2L+1)/4\pi]P_L^0(B;1,2)\ \text{Rad}_L(r_{B1},r_{B2}) \quad \text{(B12)}$$

where

$$\text{Rad}_L(r_{B1},r_{B2}) = \sum_n^{\text{shells } l=L} R_{nl}(1)R_{nl}(2)$$

is the *radial* two-particle density.

Now clearly the exchange sum of integrals can be written as

$$\sum_{m,\sigma}^{\text{fixed } L} \langle A_1B_2(m,\sigma) \mid A_3B_4(m,\sigma)\rangle = \iint dv_1dv_2a_1^*(A,1) \times \left(\frac{(2L+1)}{4\pi}\frac{P_L^0(B;1,2)}{r_{12}}\text{Rad}_L(r_{B_1},r_{B2})\right)a_3(A,2), \quad \text{(B13)}$$

and the exchange interaction of orbital pair $a_i(A)$, $a_j(A)$ with a closed-shell ion at B appears as

$$V_{i,j}^{\text{Exch}} = \sum_k^{\text{ion } B} \iint dv_1dv_2a_i^*(A,1)a_k(B,1)(1/r_{12}) \times a_k^*(B,2)a_j(A,2)$$
$$= \sum_L^{\text{ion } B} \frac{(2L+1)}{4\pi} \iint dv_1dv_2a_1^*(A,1) \times \left(\frac{P_L^0(B;1,2)}{r_{12}}\text{Rad}_L(r_{B1},r_{B2})\right)a_j(A,2). \quad \text{(B14)}$$

The operator $P_L^0(B;1,2)/r_{12}$ depends only on the relative coordinates, and can be transferred to center A directly. The radial function Rad_L can be expanded about center A in a double spherical-harmonic series, and the orthogonality of spherical harmonics reduces the expression for $V_{i,j}^{\text{Exch}}$ to a single infinite series of products of angular and radial integrals. The computation of exchange with an entire shell of (closed-shell) ions is only slightly more difficult than the two-center case. The radial integrals are identical and the angular integrals become a sum of products of rotation and vector coupling coefficients. The formulas are rather lengthy and will not be given here, but are quite easy to program for a computer.

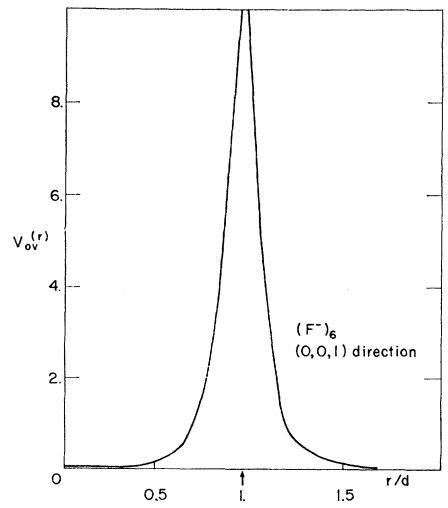

FIG. 14. $(F^-)_6$ overlap correction to its point-ion potential.